Master's thesis
Degree Programme in Materials Research
Study track

THERMORESPONSIVE POLY(N-ACRYLOYL GLYCINAMIDE-CO-METHACRYLIC ACID) MICROGELS

Heli Eronen

March 2020

Supervisor(s): Sami Hietala, Dong Yang

Examiner(s): Sami Hietala, Sirkka Liisa Maunu

UNIVERSITY OF HELSINKI
FACULTY OF SCIENCE

Faculty	Degree programme
Faculty of Science	Master's programme in materials research

Author
Heli Eronen

Title
Thermoresponsive
poly(N-acryloyl glycinamide-co-methacrylic acid) microgels

Level	Month and year	Number of pages
Pro gradu	3/2020	57

Abstract
In this thesis, thermoresponsive poly(N-acryloyl glycinamide-co-methacrylic acid) (P(NAGA-co-MAA)) microgels were synthesized via surfactant stabilized free radical precipitation polymerization. Also, PNAGA microgel was synthesized as reference. The upper critical solution temperature (UCST) behavior of the microgels was tuned by changing the molar ratio of the monomers in the copolymer. The phase transition behavior of the formed microgel particles were characterized with NMR spectroscopy, microcalorimetry, turbidimetry and light scattering.

It was observed that both PNAGA and P(NAGA-co-MAA) microgels display UCST type temperature response. However, in neutral pH, the phase transition of the copolymer gels was prevented due to the deprotonated acid groups of MAA. Hence, all the measurements were made in pH 3, below the pKa of MAA. The phase transition became sharper when the amount of MAA repeating units was increased in the copolymer. Also, the phase transition temperature of the copolymer gels increased when the amount of MAA was increased. In addition to phase transition behavior studies, the reactivity ratios of the monomers were studied during polymerization to analyze the structure of the forming copolymer gels. It was concluded that, as the both monomers had similar reactivity rates, statistical random copolymer gels are formed.

Keywords
Thermoresponsive, UCST, microgel, NAGA, MAA

Where deposited
HELDA / e-Thesis

Additional information

Table of contents

Abbreviations and symbols

AA	Acrylic acid
APS	Ammonium persulfate
BIS	N,N’-methylenebis(acrylamide)
CTAB	Cetyl trimethyl ammonium bromide
D_2O	Deuterium oxide
DLS	Dynamic light scattering
DOSY	Diffusion ordered spectroscopy
DSC	Differential scanning calorimetry
HB-UCST	Hydrogen bond derived upper critical solution temperature
LCST	Lower critical solution temperature
MAA	Methacrylic acid
NAGA	N-acryloyl glycinamide
NMR	Nuclear magnetic resonance
PAA	Poly(acrylic acid)
PMAA	Poly(meth acrylic acid)
PNAGA	Poly(N-acryloyl glycinamide)
PNIPAM	Poly(N-isopropylacrylamide)
RAFT	Reversible addition-fragmentation chain transfer
SDS	Sodium dodecyl sulfate
T_m	Melting temperature
TEM	Transmission electron microscopy
TEMED	N,N,N’,N’-tetramethylethylenediamine
UCST	Upper critical solution temperature
VPTT	Volume phase transition temperature

Introduction

The aim of this thesis was to synthesize and characterize thermoresponsive poly(N-acryloyl glycinamide-co-methacrylic acid) (P(NAGA-co-MAA)) microgels. In the literature part the reader is introduced with concepts such as thermally responsive polymers, upper and lower critical solution temperature (UCST and LCST, respectively), N-acryloyl glycinamide (NAGA) and its polymer PNAGA, methacrylic acid (MAA), microgels and surfactant stabilized free radical precipitation polymerization. The aim of the literature part is to familiarize the reader to the topic "thermoresponsive microgels", by starting with the basics of responsive polymers and moving to monomers that can be used in the synthesis. After that, the basics of microgels and surfactant stabilized precipitation polymerization, which is a commonly used method to synthesize thermoresponsive microgels, are introduced. In the end of the literature part, all the concepts are combined to explain the theory behind the synthesis of thermoresponsive P(NAGA-co-MAA) microgels.

In the experimental part, the synthesis of NAGA monomer and the synthesis of both PNAGA and P(NAGA-co-MAA) microgels are presented. A variety of characterization methods, including NMR-spectroscopy, microcalorimetry, dynamic light scattering and turbidimetry, were employed in the characterization. The results are compared and analyzed together to achieve a deeper understanding of the microgel systems. It is concluded that the UCST temperature can be tuned by incorporation of MAA. It is also noted that increasing the amount of MAA in the copolymer increases the UCST and sharpens the phase transition of the microgels. In the end of the experimental part, a short overview of interesting future studies is made.

I. LITERATURE PART

1. Responsive polymers

Smart or environmentally responsive polymers are materials which properties can be tuned by different external stimuli. These stimuli can be for example temperature[1], mechanical stress[2], pH[3], magnetic field[4] and light[5]. Typically just a small change in the environment causes a sharp change in the properties of the polymer.[6] The response can either be reversible, which means that the response can be achieved repeatedly, or irreversible which means that the polymer can be activated only once.[7] Responsive polymers are used in many applications such as catalysts[8] or use in drug delivery[9] and medical applications[10].

1.1. Thermally responsive polymers

Properties of thermoresponsive polymers can be changed by adjusting the temperature. Especially water-soluble thermally responsive polymers have gained interest as water is an environmentally friendly solvent and solvent of living systems. Water-soluble polymers must have polar groups in their structure so that they can interact with water and form dipole-dipole and hydrogen bonds. Usually a small change in temperature causes a huge change in the solubility properties of the polymer.[1] This can be used in smart applications including drug delivery and release applications[11], switchable hydrophilic-hydrophobic surfaces[12] and catalysts[13]. In this thesis only water-soluble polymers, which phase behavior is based on hydrogen bonding, are studied in detail. These are chosen as they are usually thermally responsive in aqueous solutions under physiological conditions. Also, the synthesis and tuning the phase transition temperature should be rather easy.[1] If the phase behavior isn't based on the hydrogen bonding it is usually based on ionic interactions. The ionic interactions are, however, sensitive to salt which makes them difficult under physiological conditions.[14] Hence, the polymers based on hydrogen bonding are focused in this thesis.

Two main categories are defined based on the behavior of polymer upon change in the temperature. Polymers which phase separate upon heating display lower critical solution temperature (LCST) and polymers which phase separate upon cooling display upper critical solution temperature (UCST) in their phase diagram.[1] The simplified phase diagram of LCST and UCST polymers is presented in Figure 1a. In the Figure 1a, the phase diagram is sketched so that the temperature is plotted as a

function of solute concentration. The definition of LCST and UCST states that the polymer is miscible with the solvent in all concentrations below the LCST and above the UCST. Therefore, the LCST and UCST are the exact points in the phase diagram where the curves reach to their minimum or maximum, respectively. The other points on the curves are usually called transition temperatures, and for microgels volume phase transition temperatures (VPTT). These points are concentration dependent and express the boundaries of the phases in equilibrium.[1] The Figure 1a only presents the ideal, symmetrical, phase diagram. In real cases nonsymmetrical, as for example in case of polystyrene in cyclohexane[15], bimodal, as in case of polystyrene in acetaldehyde[16], almost flat curves, as in case of poly(methyl methacrylate) in n-butanol[17] or PNIPAM in water[18], or closed phase separation loops called miscibility loops, as in case of polyethylene glycol in water[19], can exist. A schematic presentation of different phase diagrams is presented in Figure 1b.

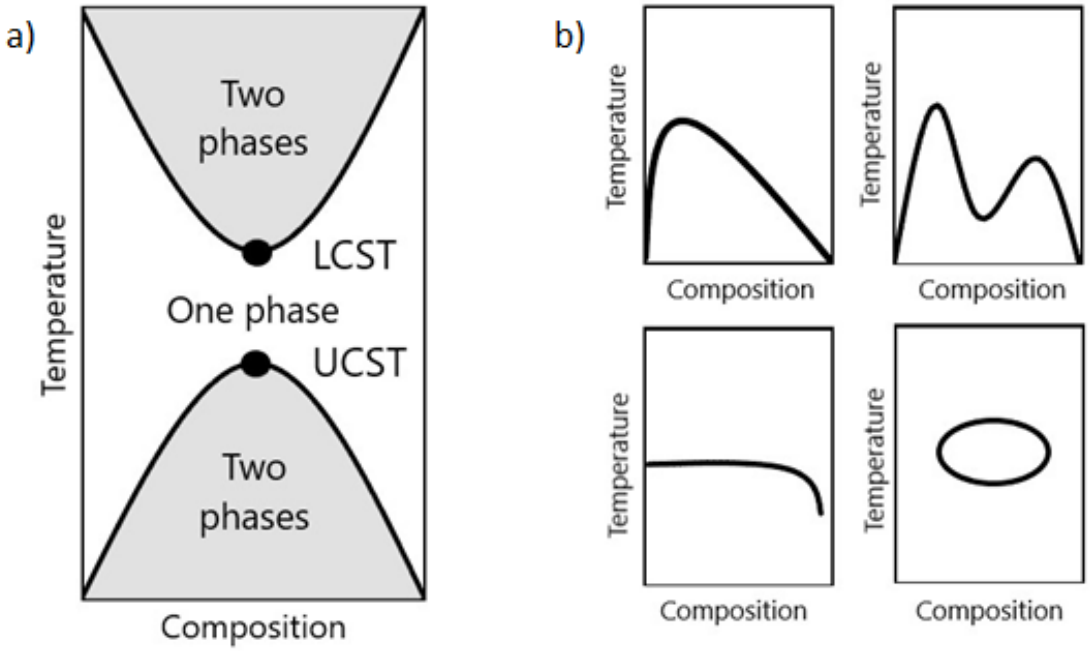

Figure 1. a.) The ideal phase diagram of LCST and UCST polymers. LCST polymers phase separate upon heating and UCST polymers phase separate upon cooling. b.) Schematic presentation of some possible phase diagrams including asymmetrical, bimodal, flat and loop.

Polymers with lower critical solution temperature behavior have been studied widely. Between 2010-2018, an average of 460 publications per year involved “LCST” (Scifinder, word search, 2010-2018, 28.8.2019). On the other hand, polymers with upper critical solution temperature behavior have not been studied as extensively as LCST polymers. Between 2010-2018, an average of 82 publications per year involved “UCST” (Scifinder, word search, 2010-2018, 28.8.2019). As seen from Figure 2, the amount of LCST containing publications has been rather stable during the 2010s but the amount of publications containing UCST has increased significantly. Indeed, UCST polymers are an interesting topic having still much to research.

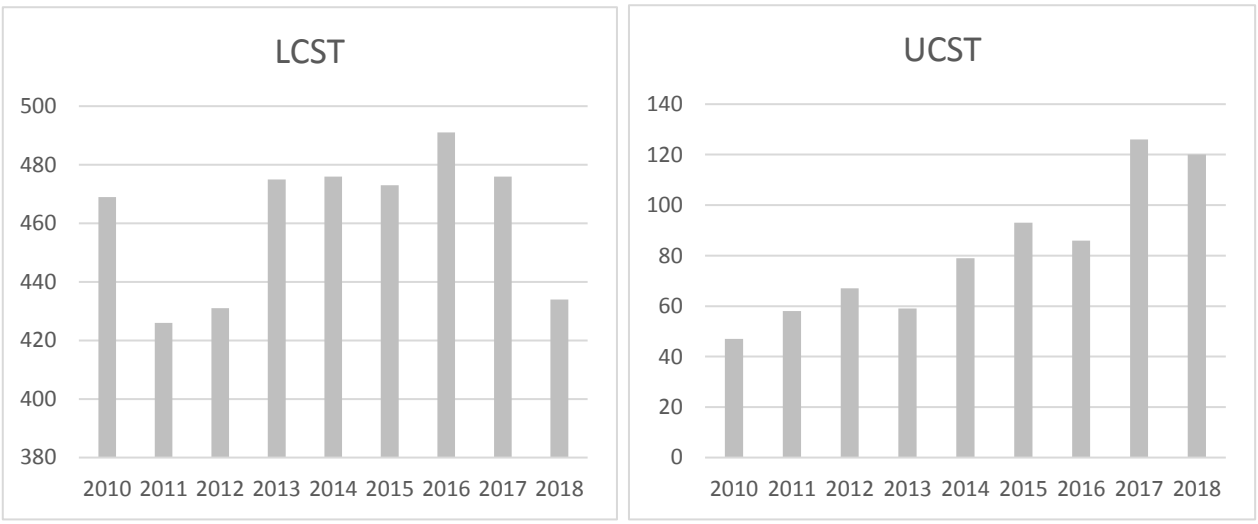

Figure 2. The number of publications containing topic “LCST” or “UCST” between the years 2010-2018 (Scifinder, word search, 2010-2018, 28.8.2019). Note the difference in y-axis. The amount of LCST publications has been quite stable but the amount of UCST publications has increased significantly.

1.1.1. Poly(N-isopropylacrylamide)

Polymers which precipitate upon heating have lower critical solution temperature (LCST) behavior.[1] The most commonly studied LCST polymer is poly(N-isopropylacrylamide) (PNIPAM), Figure 3.[20] PNIPAM was first synthesized in 1956 by Sprecht et al.[21] A bit over ten years later, in 1968, Henskin et al. published the paper focusing on the phase behavior of the PNIPAM. In this publication they found out that the LCST temperature of PNIPAM in aqueous solutions is around 31 °C.[22] Nowadays the LCST temperature of PNIPAM is usually cited to be 32 °C.[20] In the case of PNIPAM in aqueous

solution, the LCST behavior is based on hydrogen bonding between the amide group and water. The amide group is protected by hydrophobic isopropyl group. When the amide group forms hydrogen bond with water molecule a small displacement in the isopropyl group occurs allowing more water molecule bonding which eventually causes the water solubility of the polymer. Heating of the solution causes dehydration and collapses the chain to globule. The hydrogen bonding also causes the flat shape of the phase diagram as mentioned in section 1.1.[18] Even the polymer is known for a quite a long time it is still studied extensively in these days. An average of 1052 publications per year have been dealing the topic "poly(N-isopropylacrylamide)" in the 2010s (scifinder, word search, 2010-2018, 19.11.2019). This indicates the importance of thermoresponsive polymers and the interest towards the topic.

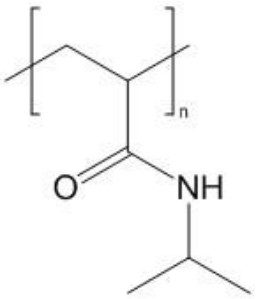

Figure 3. Structure of poly(N-isopropylacrylamide) (PNIPAM), the most commonly studied LCST polymer.

2. Upper critical solution temperature (UCST)

Upper critical solution temperature (UCST) polymers precipitate upon cooling. Polymers having UCST behavior in water are known but many do not have the behavior in saline solution or physiological conditions.[1] To be usable for applications, the phase transition should be stable and sharp and only slightly dependent on external stimulations, as for example concentration and pH. For these requirements, hydrogen bonding UCST (HB-UCST) polymers have been noted to be promising candidates.[23] It has been also shown that if the UCST behavior is based on hydrogen bonding the VPTT is less sensitive to the presence of electrolytes or the changes in solution concentration.[24] Hence, this thesis focuses on the HB-UCST polymers. In theory, to create a HB-UCST

polymer that has a UCST behavior which fulfills all the requirements mentioned above, a list of functions should be incorporated to the polymer. First, the hydrogen bonding should be strong, which could be achieved by incorporating strong hydrogen bond donors and acceptors.[23] A primary amide group can act as a hydrogen bond donor and it seems to appear in all known UCST polymers. Hence, it is often thought to be the most relevant functionality to create reversible hydrogen bonding.[24] Second, there should be no ionic groups in the polymer as they can prevent the UCST behavior. Third, the polymer should be stable in water solutions so that the phase transition would be sharp and reversible. And fourth, if copolymerization is used, the composition of the copolymers should be rather similar in all chains.[23] A polymer consisting all these functions has been synthesized by Seuring et al. by copolymerizing acrylamide and acrylonitrile.[24] The structure of acrylamide is presented in Figure 4. Acrylamide was used as it is a simple monomer having the primary amide group and acrylonitrile was used as a comonomer to modify the hydrophilicity of the polymer. It was found out that the copolymer indeed showed sharp UCST behavior and that the VPTT of the copolymer could be tuned by changing the copolymer composition.[24] In this case the primary amide group acts as a hydrogen bond donor and the carbonyl group acts as a hydrogen bond acceptor. Other polymers having similar structures can also have UCST behavior. From these, the best example is one of the most studied UCST polymer called PNAGA.[23] The monomer NAGA and the polymer PNAGA are introduced thoroughly in the following sections.

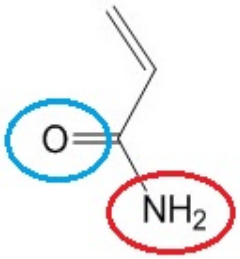

Figure 4. Structure of acrylamide. The primary amide group, marked with red circle, acts as a hydrogen bond donor and the carbonyl group, marked as a blue circle, acts as a hydrogen bond acceptor.

2.1. N-acryloyl glycinamide and poly(N-acryloyl glycinamide)

Synthesis of N-acryloyl glycinamide (NAGA) was first published in 1964.[25] Hence, the monomer and its polymer (PNAGA) are known already for fifty-five years. PNAGA is a non-ionic polymer which has two amide groups which can act as hydrogen bond donors and two carbonyl groups which can act as hydrogen bond acceptors. The structures of the NAGA and the PNAGA are presented in Figure 5.[14] PNAGA has an upper critical solution temperature (UCST) behavior in water. The hydrogen bonds cause the UCST behavior of the PNAGA in an aqueous solution.[14] When the phase transition happens and the polymer precipitates, the polymer-polymer hydrogen bonds form and polymer-water hydrogen bonds break. Inversely when the polymer dissolves the polymer-polymer and water-water hydrogen bonds brake and polymer-water hydrogen bonds form.[1] The phase transition of PNAGA happens in wide temperature range as the phase transition depends on many parameters such as ionic end groups, concentration and molar mass. Phase transition values from 0 °C to 30 °C are reported at different conditions.[26] For example a phase transition temperature of a 1.0 w% solution of carefully purified PNAGA is reported to be 22-23 °C.[14] Even a small amount of ionic groups can prevent the UCST behavior of PNAGA and hence the preparation, and especially the purification of the monomer, should be done carefully.[14] The purity of the monomer can be verified by determination of melting point. The melting point can be determined by using differential scanning calorimetry. The previously reported melting points for the NAGA monomer are 129 °C[25], 136-136.5 °C[27], 137-139 °C[26] and 143 °C[14] depending on the amount of impurities.

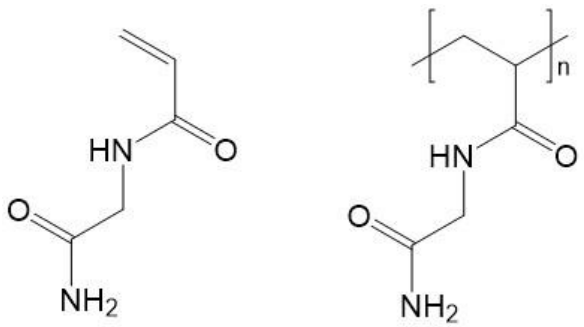

Figure 5. The structures of NAGA and PNAGA. The two amide groups can act as hydrogen bond donors and the two carbonyl groups can act as hydrogen bond acceptors.[14]

2.1.1. Synthesis of N-acryloyl glycinamide monomer

The synthesis of NAGA, according to Haas et al., is presented in Figure 6.[25] The mechanism they proposed for the synthesis is later modified to minimize the formation of potassium acrylate as a side product. If potassium acrylate is present during polymerization, acrylic acid will be incorporated to the polymer. The carboxyl groups in the polymer backbone suppress or even prevent the UCST behavior. In the modified synthesis the amount of acryloyl chloride is reduced as it was used in excess in the original synthesis. Also, in the original synthesis the potassium carbonate solution was added to the mixture of glycinamide hydrochloride and acryloyl chloride, which causes the acryloyl chloride to hydrolyze to potassium acrylate. In the modified synthesis the acryloyl chloride is slowly added to the glycinamide solution to minimize the formation of potassium acrylate. The purification of the product is highly important to achieve both potassium salt and acrylate free monomer.[14]

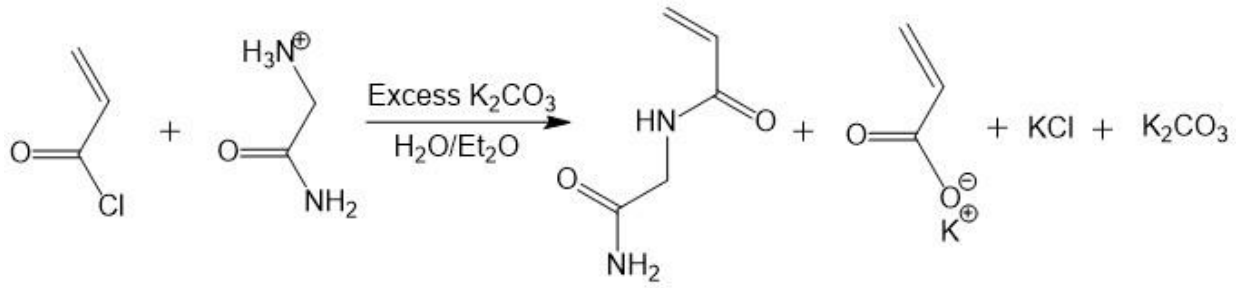

Figure 6. Synthesis of N-acryloyl glycinamide according to Haas et al.[25]

2.2. Modification of the UCST

So, the reported phase transition temperatures of PNAGA vary from 0 °C to 30 °C depending on the amount of impurities and the properties of the polymer including for example the molar mass.[26] As for example the normal temperature of the human body is usually thought to be around 37 °C, the listed phase transition temperatures of PNAGA are rather low for biological applications. Hence, the modification of the UCST of the PNAGA has been studied. As the phase transition behavior of the PNAGA is based on hydrogen bonding, strengthening the hydrogen bonding could be used to increase the UCST. It is noted, that copolymerization with proper comonomer, that bears a

hydrogen bond donor or acceptor in its structure, can be used to increase the UCST.[28] According to reported results, copolymerization of NAGA with acrylonitrile[29] or methacrylic acid[28] increases the UCST up to 40 °C. In case of acrylonitrile copolymerization it was noted that acrylonitrile sharpened and increased the UCST of the copolymer compared to PNAGA polymer. Also, the hysteresis between heating and cooling decreased and the copolymer was found out to be more resistant to changes in solution and electrolyte concentrations.[29] However, due to the toxicity of the acrylonitrile, other comonomers have also been studied. Wenhui et al. synthesized P(NAGA-co-MAA) copolymer by reversible addition-fragmentation chain transfer (RAFT) polymerization of methacrylic acid (MAA) and NAGA. The molar fraction of MAA was from 1 % to 59% and the copolymers were studied in aqueous solutions at pH 4 and at pH 1. They concluded that MAA increased the UCST of the copolymer compared to homopolymer. The UCST increased from 10 °C up to 65 °C when the amount of MAA increased from 1 % to 59 % when measurements were made in pH 1. When the similar measurements were made in pH 4 the UCST increased from 4 °C to 38 °C.[28] As MAA seems a good candidate to increase the UCST of linear PNAGA, it was used in this thesis for preparation of microgels.

2.2.1. Methacrylic acid

Methacrylic acid (MAA) is an anionic monomer due to a carboxylic acid group in the structure and therefore poly(methacrylic acid) (PMAA) is an anionic polyelectrolyte.[30] PMAA is weakly acidic with the pKa value of approximately 4.7.[31] Hence, the polymer is mainly in the anionic form in a neutral pH. The structures of both MAA and PMAA are presented in Figure 7. Due to the methyl group in the polymer backbone the PMAA is more hydrophobic than for example poly(acrylic acid) (PAA) and it forms complexes with the polymers that have hydrogen bond acceptors in their structure.[30] Hence, MAA can be used as a comonomer in copolymer synthesis to modify the hydrophilicity of an UCST polymer.[28] When the pH of the polymer solution is lowered below the pKa value, PMAA is rather hydrophobic as the acid groups are protonated and there are no charges present. Conversely, when the pH is above the pKa value, the acid groups are deprotonated, and the hydrophilicity of the polymer is increased. Also, the anionic groups create repulsive forces which increase the swelling of the polymer.[32] Thus, by changing the pH, the hydrophilicity and therefore the UCST of the copolymer can be tuned.

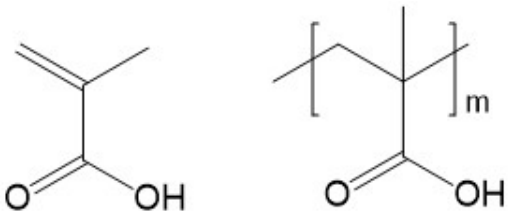

Figure 7. Structures of methacrylic acid and poly(methacrylic acid). The carboxylic acid group makes the compounds anionic in neutral pH.[28]

3. Microgels

Microgels in aqueous solutions are usually spherical particles with a diameter from 20 nm to 50 µm. The particles are constructed by crosslinked polymer chains and the polymer network is swollen by solvent.[9] However, the definition of microgel is not universal and for example the definition of the size of the microgel varies in literature.[9,33,34] Still, some characteristic properties can be listed. First, microgel particles have particle size distribution. Second, the particles form stable dispersion in aqueous solution as they are stabilized by the hydrogen bonding with water. Third, microgels have an average crosslinking density, which depends on the used amount of crosslinking agent. And fourth, microgels degree of swelling depends on the interactions between polymer-polymer and polymer-water and the conditions of the surrounding medium, including for example pH and temperature. By concluding all these properties, microgels in aqueous solutions can be thought to be spherical solvent swollen polymer networks in a microscopic scale that changes their properties, including size and density, when the surrounding conditions are changed.[33] So, in a way, microgels combine properties which are usually known as properties of aqueous polymers, aqueous macrogels and hydrophobic latex-particles, as the properties of the microgel depend on polymer-polymer and polymer-water interactions as in case of aqueous polymers, and, they are defined by the degree of swelling and crosslinking density as in case of macrogels. As the microgels have the particle size distribution in colloidal domain they can be studied by light scattering methods and rheology.[34] As the microgels combine properties of so many different systems, they are indeed very interesting subject to research.

One important class of microgels are thermally responsive microgels. They are interesting as they combine the versatile properties of both thermoresponsive polymers and microgels. Usually, if a

linear polymer is thermally responsive it can be crosslinked to achieve thermoresponsive microgel.[34] Different ways to crosslink a polymer are introduced next.

3.1. Crosslinking

A first study about the gelation of polymers was done by Carothers already in the 1931. In his work, he did polycondensation reactions with multifunctional monomers and resulted three-dimensional networks.[35] Since that, many methods have been developed to create polymer gels including not only reactions with different multifunctional crosslinkers but also many novel methods including both chemical and physical crosslinking.[36] The chemically crosslinked gels are usually more stable than physically crosslinked due to the stability created by covalent bonds.[32] Overall, chemical crosslinking, done in radical polymerization by crosslinking agent, is a commonly used method to synthesize microgels.[36] Hence, this method is discussed in more detail.

3.1.1. Chemical crosslinking in radical polymerization

One method to synthesize chemically crosslinked microgels is radical polymerization in the presence of crosslinker.[36] Often used crosslinking agent is N,N,-methylenebis(acrylamide) (BIS), Figure 8.[33]

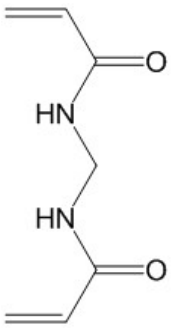

Figure 8. The structure of N,N,-methylenebis(acrylamide) (BIS).[8]

During radical polymerization, the carbon-carbon double bonds from the BIS react in the same way as the double bond from the monomer, resulting in crosslinked structure between the polymer chains. However, according to the studies by Wu et al. done already in the 1994, BIS crosslinker reacts faster than the commonly used LCST polymer PNIPAM.[37] This causes an uneven density of the formed microgel particles in the swollen state, where the core is denser due to higher amount of crosslinker and the density decreases when the distance from the core increases.[38] Hence, the microgel particles usually show fuzzy structure in the swollen state as the highest polymer density is located in the core. The overall density of the particles in tuned by changing the amount of crosslinking agent in the synthesis. A schematic presentation of fuzzy microgel particle in the swollen state is presented in Figure 9.[39]

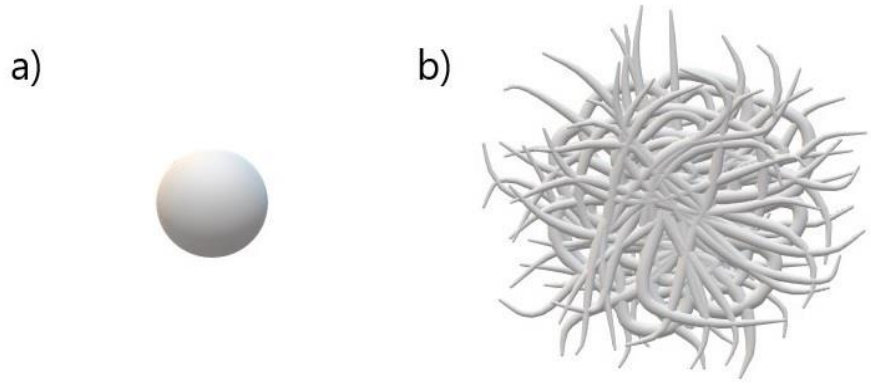

Figure 9. A schematic presentation of microgel particle in a.) collapsed state and b.) swollen state. The particle is in collapsed state below the VPTT of UCST behaving polymer and in swollen state above the VPTT. As the crosslinking agent, BIS, reacts faster than the monomer, the particle density decreases when the distance from the core increases. This causes a fuzzy structure in the swollen state.[39]

If persulfate initiation system is used, crosslinks can be formed even in the absence of crosslinking agent.[40] This is called peroxide crosslinking and it is caused by chain transfer reactions which can happen during the polymerization.[41] Both peroxide crosslinking and BIS crosslinking can happen at the same time.[42] When a radical is transferred to a polymer chain, it creates a radical site that can

react with the monomers in the solution. A network structure can be formed if a coupling termination between formed side chain and another chain occurs. The formation of self-crosslinks is presented in Figure 10a. However, if redox initiation system is used, instead of peroxide initiation, no peroxide crosslinking occurs. One well known redox system is ammonium persulfate (APS) and N,N,N',N'-tetramethylethylenediamine (TEMED).[42] In redox system, TEMED acts as a transfer reagent and diminishes peroxide crosslinking as chain transfer with TEMED is preferable.[43] The chain transfer with TEMED is presented in Figure 10b. So, different network structures are formed depending on the initiation system.

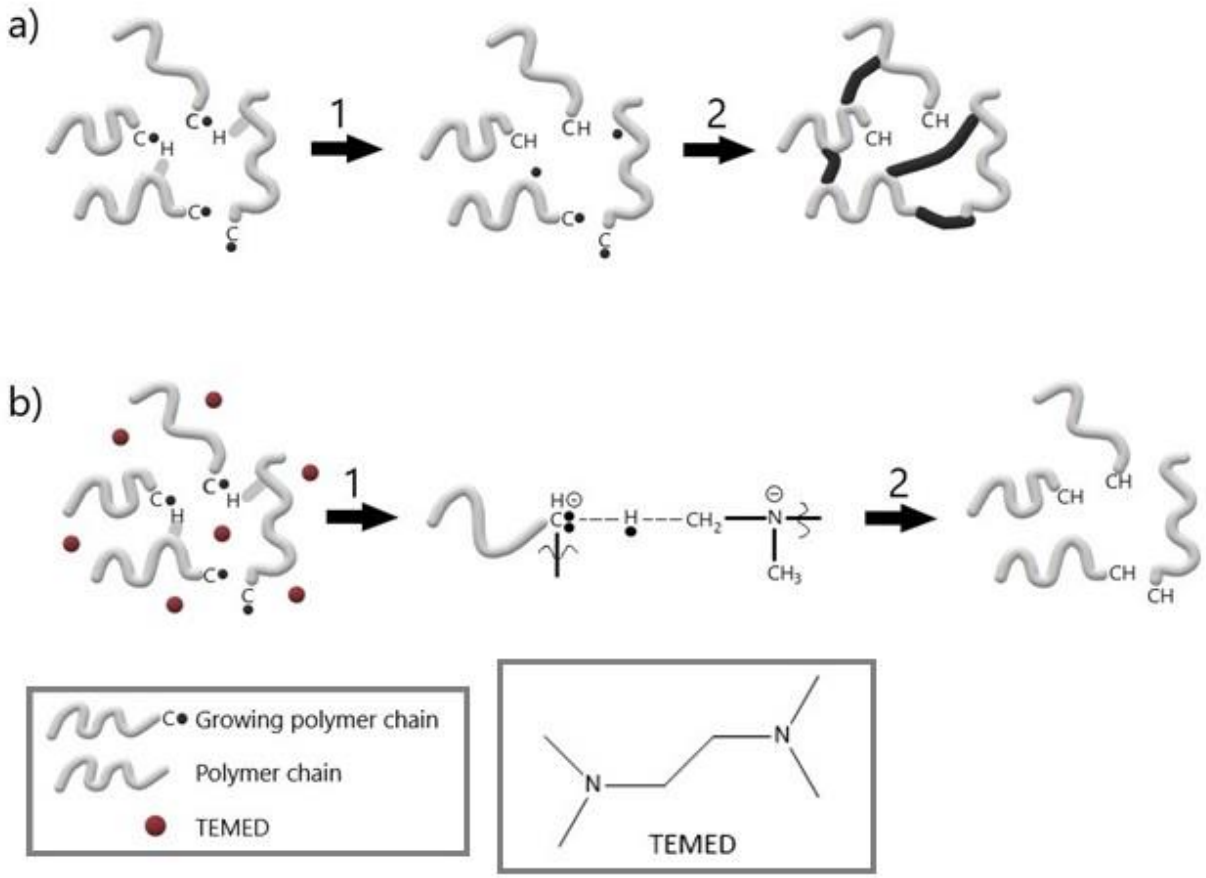

Figure 10. Schematic presentation of the self-crosslinking and how TEMED prevents it. a.) Step 1: chain transfer reactions, where radical sites are created. Step 2: Chains grow to radical sites due to addition of monomers. If termination happens by coupling, network is created. b) Chain transfer reactions with TEMED prevents the chain transfer between polymers and no network is formed.

4. Free radical precipitation polymerization

Free radical precipitation polymerization is a widely used method to synthesize water dispersible thermoresponsive microgels. In this method, microgels are formed by vinyl addition copolymerization reaction of monomers and crosslinking agents. The reaction is initiated by a system that creates free radicals. The reaction takes place in heterogeneous phase as all the ingredients are soluble in water at the beginning of the reaction, but as the reaction proceeds the polymers precipitate due to the thermoresponsive behavior. The precipitation is achieved when the polymerization temperature of the UCST polymer is kept below the UCST. This causes the polymer precipitation due to strong hydrogen bonding between polymers.[32] In precipitation polymerization, many properties of the microgel particles can be controlled. These are for example the size and the size distribution, the surface properties and the architecture of the particles.[33] For PNIPAM it has been shown that the size of the microgel particles can be tuned from tens of nanometers to few micrometers by addition of surfactant.[44] Also, particles with narrow size distributions can be created. The architecture of the particles can be tuned by for example copolymerization or incorporation of nanoparticles. Another advantage is that different polymerization processes can be used, including for example batch, semi-batch and continuous feeding. This allows the tuning of the reaction and hence more precise formation of particles.[33] It is known that all conditions, including temperature, choice of initiator, concentration of the different ingredients and rate of stirring, affect to both to the volume and aggregation of the created particles.[40]

4.1. Initiation

In the beginning of the precipitation polymerization all ingredients are soluble in water. Many water-soluble initiators can be used including peroxide and azo-based initiators.[33] In many cases the redox initiation is used. One redox initiating system is ammonium persulfate (APS) and N,N,N',N'-tetramethylethylenediamine (TEMED), which is commonly used in low temperature polymerizations.[45] When TEMED and APS are mixed together the tertiary amine group from TEMED reacts with APS and creates radicals which then initiate the polymerization reaction. The reaction between APS and TEMED is presented in Figure 11. At high temperatures or long reaction times the peroxydisulfate can also dissociate itself into free radicals and thus initiate the reaction.[46]

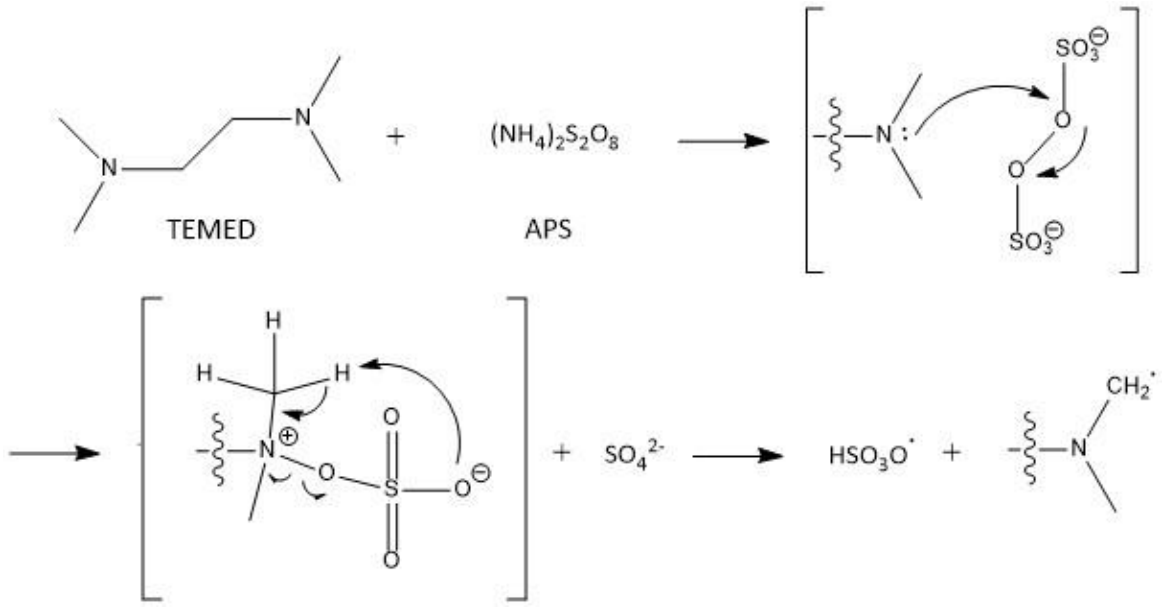

Figure 11. APS and TEMED redox initiation system mechanism. Tertiary amine group from TEMED catalyzes the reaction in low temperatures.[46]

4.2. Propagation

In free radical precipitation polymerization for thermally responsive polymers the formation of particles starts with the formation of precursor particles. When the reaction proceeds and the chain length increases to critical length, the chain collapses and forms the precursor particle. This is due to the precipitation as the polymerization is done below the phase transition temperature of the UCST polymer. The formed precursor particles can grow in different ways. Addition of monomers grows the particle, but the particles can also aggregate and form larger polymer particles. In addition to aggregation by themselves, the precursor particles can also attach to the surfaces of polymer particles that are already existing in the solution. After the microgel particles have reached to the critical size, the electrostatic forces stabilize them to colloidal stable particles. The electrostatic forces are based on the sulfate groups from the persulfate initiator or surfactant. The sulfate groups are associated in the polymer while the microgel particles form and grow.[33,34] If microgel particles with small size are wanted, more efficient stabilization is needed. This can be achieved by addition of ionic surfactant which stabilizes the formed precursor particles and hence smaller particles are formed. Inversely, decreasing the amount of added surfactant leads to the formation of bigger

particles as the precursor particles are not stabilized well.[47] The effect of surfactant is discussed more detailed in the next section. The stabilized particles have a large amount of water in their structure even in the collapsed form. Microgel particles are collapsed below the VPTT. When temperature is increased over the VPTT of the UCST behaving polymer, the polymer network swells. In the swollen state the particles are stabilized by hydrogen bonds between water and the polymer. The precipitation mechanism is presented in Figure 12.[33,34]

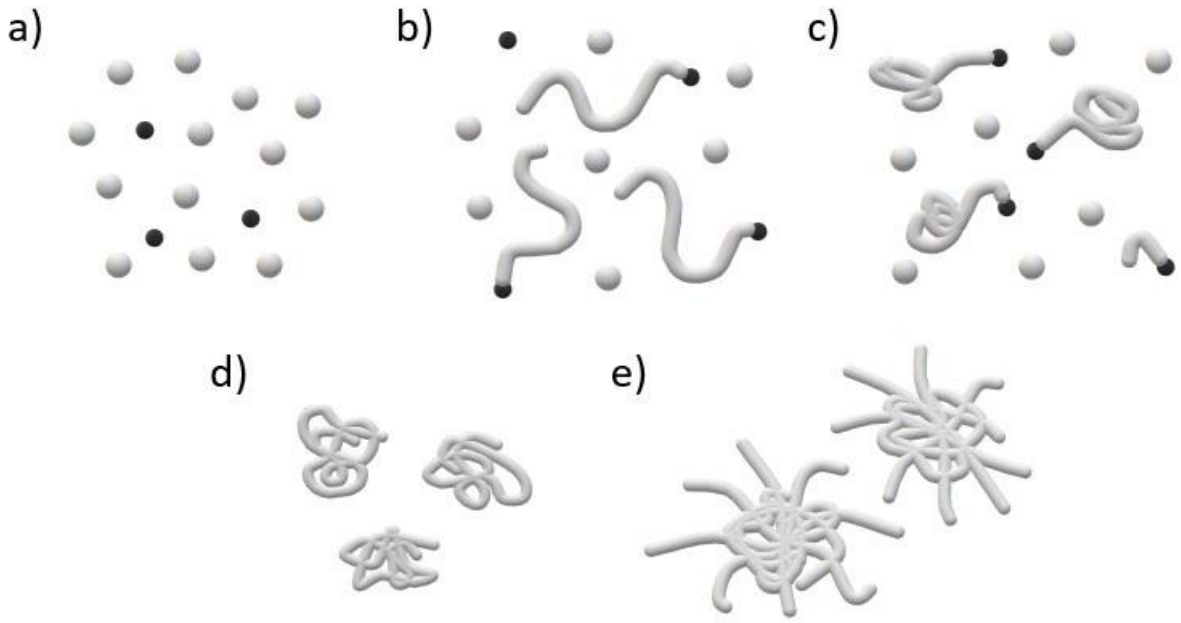

Figure 12. Mechanism for precipitation polymerization. a.) Monomers (grey dots) and initiator (black dots) are freely in the solution b.) Chains grow c.) Precursor particle is formed when the chain reaches the critical length d.) Precursor particles can grow in different ways, as for example by addition of monomers, aggregation with other precursor particles or aggregation with already existing polymer particle e.) Formed microgel particles adopt swollen morphology above the VPTT of the UCST behaving polymers.[33,34]

4.3. Surfactant stabilized microgels

During the precipitation polymerization the electrostatic forces, created by the ionic initiators, stabilize the precursor particles. However, the stabilization efficiency of the ionic initiator residuals is not strong. Hence, microgel particles, created by surfactant free method, are usually large and show wide variation of particle sizes. In surfactant stabilization, surfactant is added to the solution. One widely used surfactant is sodium dodecyl sulfate (SDS). The surfactant stabilizes the formed precursor particles and prevents them from aggregating, which leads to the formation of smaller particles with narrower size distribution.[33] More precise formation of particles is needed when particles are created for some specific application. For example, it has been noted that nanoparticles, which have a size smaller than 100 nm, are more potential candidates for drug delivery systems than bigger ones due to the extendable circulation time.[48] Hence, controlling the particle size is an important thing to be considered.

Pelton et al. studied the effect of surfactant stabilization already in 1993.[44] In their work, they synthesized PNIPAM microgels with the presence of SDS. They noted that the size of the microgels at 25 °C decreased by a factor of 10 when SDS was used in the synthesis. They showed that already low concentration of SDS stabilizes particles effectively, as they used SDS with the concentration range from 0.2 mmol to 4 mmol. They also noticed that above the concentration of 2 mmol of SDS, the hydrodynamic diameter of the particles stays constant.[44] Since that, many have been studied the stabilization effect of surfactants. For example, Arleth et al. synthesized PNIPAM nanogels with high concentration of SDS. They used 5.3 mmol of SDS in their synthesis and got homogeneous nanogel particles with the radius less than 50 nm at 25 °C.[49] Also Andersson et al. have studied the stabilization effect of SDS to the PNIPAM microgels. They used SDS with the concentration range of 0.4-6.7 mmol. They concluded, similarly as Arleth et al., that when the concentration of SDS is increased the hydrodynamic size of the microgel particles decreases and the homogeneity of the particles increases. They also concluded that high concentration of SDS affects to the structure of the microgel as the surfactant prevents the PNIPAM to aggregate tightly. If PNIPAM would be able to pack during the precipitation, it could eventually lead to formation of solid, crosslinked, PNIPAM particles. But as the large amount of SDS prevents the packing, it changes the system to resemble more of a good solvent conditions and hence, prevents the solid PNIPAM particle formation. This leads to the decrease in turbidity in good solvent conditions when the amount of SDS is increased.[50] The stabilization can be also achieved by addition of other surfactants, including for example cetyl

trimethyl ammonium bromide (CTAB)[51], or by changing the ionic strength of the reaction solution[52]. Also, for example copolymerization with monomers bearing ionic groups can be used to stabilize the particles.[53] As the stabilization is based on addition of ionic charges, changing the charge density of the particles in any way should affect to the final size of the particles.[40]

5. Synthesis of USCT type microgels

PNAGA is a thermoresponsive UCST type polymer. According to literature, also NAGA microgels can be synthesized. Yang et al. synthesized PNAGA microgels via precipitation polymerization. They used BIS as a crosslinker, SDS as a surfactant and APS and TEMED initiation system and did the polymerization in 0 °C, which is below the UCST of PNAGA, to achieve the precipitation. They got thermoresponsive aqueous microgels and successfully showed that silver nanoparticles can be loaded inside the microgel particles and released by changing the temperature. Hence, PNAGA microgels can be used as catalysts.[8] Sun et al. synthesized thermoresponsive linear P(NAGA-co-MAA). They copolymerized NAGA and MAA via RAFT polymerization and noted that by increasing the amount of MAA in the copolymer the UCST of the copolymer can be increased.[28] As the PNAGA microgels can be used in catalysis and MAA have been noted to increase the UCST of the linear PNAGA, it would be interesting to combine these properties by synthesizing and characterizing the copolymer microgels. Overall, as thermoresponsive microgels can be used in many applications, as biosensors[54], emulsion stabilizers[55], drug delivery[9] and nanocatalysis[8], they are an interesting and important topic to be studied.

II. EXPERIMENTAL PART

6. Introduction

The aim of this research was to synthesize poly(N-acryloyl glycinamide) (PNAGA) UCST micro/nanogels with tunable phase transition temperature. The phase transition temperature was tuned by using methacrylic acid (MAA) as a comonomer in the polymerization. P(NAGA-co-MAA) microgels were prepared by surfactant stabilized free radical precipitation polymerization. The polymerization was initiated by APS and TEMED redox system in the presence of surfactant (SDS) and crosslinker (BIS) to achieve stabilized particles and crosslinked structure. The APS+TEMED redox system was used as TEMED initiates the reaction in low temperatures, prevents the self-crosslinking and stabilizes the particle volume when temperature is changed.[40] The polymerization temperature was kept below the VPTT of the PNAGA to achieve the precipitation. The main mechanism of the formation of P(NAGA-co-MAA) microgels is presented in Figure 13. As seen already in the Figure 11, APS decomposes and forms radicals. These sulfate radicals react with water-soluble monomers which leads to radical propagation and chain growth. Reaction with two functional crosslinking agent causes the crosslinked structure.[33]

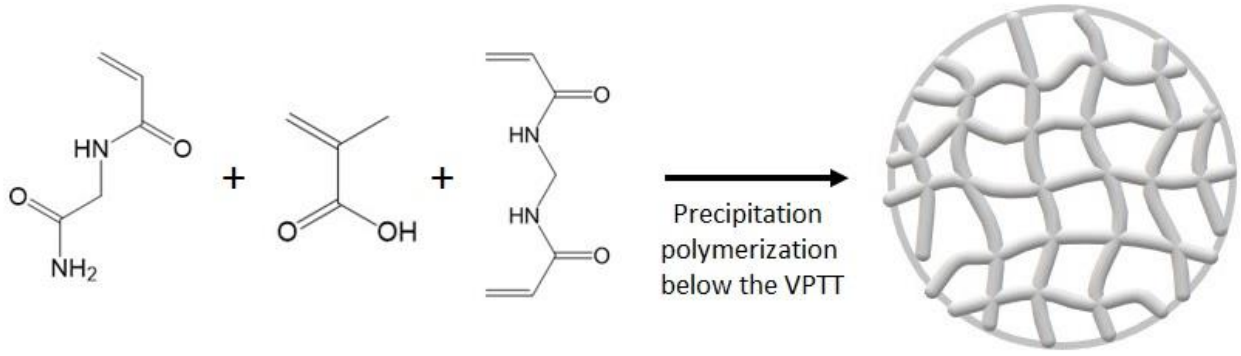

Figure 13. The formation of P(NAGA-co-MAA) microgels. The sulfate radical from APS reacts with the double bonds from monomers and crosslinking agent creating a crosslinked structure during the precipitation polymerization which is done below the VPTT of the UCST type polymer.

In case of P(NAGA-co-MAA) polymer the modification of the UCST is done by strengthening the hydrogen bonding.[28] As the MAA is a hydrophilic monomer, the amount of MAA could be limited so

that an effective precipitation is achieved during the copolymerization. This is because the precipitation of the copolymer during the polymerization depends on the hydrophilicity of the formed copolymer. If the forming precursor particle is too hydrophilic, it will not undergo effective precipitation which can lead to the formation of uneven dispersion or even no particle formation.[47] So, synthetization of P(NAGA-co-MAA) microgels poses many interesting aspects and questions to be studied.

First N-acryloyl glycinamide (NAGA) monomer was synthesized and then the PNAGA microgel was prepared. The PNAGA microgel was used as a reference for the copolymer gels. The copolymer gels P(NAGA-co-MAA) were made with different monomer ratios. The amount of MAA in the monomer feed was tuned to be 10 %, 30 %, 50 % and 70 %. In this thesis, following naming is used: "10 % product" refers to the copolymer sample with the molar ratio of 10 % of MAA, "30% product" to the copolymer with 30% of MAA etc.

Many methods were used to analyze the products. DSC measurement was used to define the purity of the synthesized NAGA monomer. NMR measurements were made to determine the conversions. Also, the purity of the microgels were determined via NMR measurements. NMR measurements with multiple temperatures were used to follow the phase transition behavior of the microgels as a function of temperature. The multiple temperature NMR measurements were also made at pH 3 to study how the pH affects to the phase transition behavior. The results were compared with calorimetric data. Reaction kinetics were followed with NMR measurements to predict if random copolymers are formed. Light scattering measurements were made to determine the size of the prepared microgel particles and to follow the size as a function of temperature. Turbidity measurements were made to determine the temperature where the visual change happens.

7. Materials

Glycinamide hydrochloride (Bachem), potassium carbonate (Fischer Scientific), acryloyl chloride (Sigma Aldrich), anhydrous diethyl ether (J.T. Baker), acetone and methanol (both from Sigma Aldrich) were all used as received to prepare N-acryloyl glycinamide (NAGA) monomer according to the procedure described in the literature.[26] N,N,N',N'-tetramethylethylenediamine (TEMED) and sodium dodecyl sulfate (SDS) (both from Sigma) were used as received. Recrystallized ammonium persulfate (APS) and N,N'-methylenebis(acrylamide) (BIS) and distilled methacrylic acid (MAA) were

used in the polymerization. Deionized water was used in the syntheses and in purifications of the products. A dialysis membrane with a molecular weight cutoff of 12-14 kD was used for the purification.

8. Syntheses

8.1. Synthesis of N-acryloyl glycinamide

The monomer N-acryloyl glycinamide (NAGA) was synthesized according to the literature.[26] First glycinamide hydrochloride (3 g, 27.14 mmol) and potassium carbonate, K_2CO_3, (7.5 g, 54.26 mmol) were dissolved together in 50 ml of deionized water in a 250 ml three-necked round bottomed flask. The solution was cooled down in an ice bath. Acryloyl chloride (2 ml, 24.73 mmol) was diluted with 100 ml of an anhydrous diethyl ether and added dropwise to the cooled solution within 30 minutes under vigorous stirring. After the addition, the ice bath was removed, and the stirring was continued at room temperature for two hours. After two hours the ether phase was separated from the water phase and the remaining water solution was freeze dried. The synthesis of crude NAGA was repeated ten times. All the crude products were added to a 1000 ml beaker with 900 ml of acetone and stirred at 40 °C for eight minutes. The mixture was filtered to separate the non-soluble potassium salts. The extraction with acetone was repeated six times. Most of the acetone was removed by rotary evaporator at 40 °C. The precipitated crude NAGA was filtered and then dissolved to 1750 ml of acetone in 2000 ml beaker at 55 °C. The dissolved solution was filtered and placed into a freezer (-30 °C) overnight. The crystallized product was filtered and dissolved to 170 ml of methanol:acetone (1:2) mixture at 55 °C. The product was recrystallized in freezer and filtered. The recrystallization was repeated to increase the purity: the product was added to the 400 ml beaker and 140 ml of methanol:acetone (1:2) mixture was added at 55 °C to obtain a full dissolution. The solution was then placed at -30°C and the formed crystals were filtered and dried under vacuum overnight to achieve the pure NAGA monomer.

8.2. Synthesis of poly(N-acryloyl glycinamide) microgel

The synthesis of poly(N-acryloyl glycinamide) (PNAGA) microgel adopted from the literature[8] was used for all the microgels prepared in this project. The amount of BIS was 3% of the amount of monomer.

First NAGA (449.09 mg, 3.50 mmol), BIS (16.27 mg, 0.11 mmol) and SDS (57.61 mg, 0.20 mmol) were added to a 100 ml round bottomed flask with magnetic stirrer bar and the flask was purged with nitrogen for 40 minutes. 50 ml of deionized water was added to another flask and purged also with nitrogen. After 40 minutes, the purged water was transformed to the 100 ml round bottomed flask and the flask was placed in an ice bath. The purging was continued for another 40 minutes. An NMR sample was taken after a full dissolution of the solid materials. The reaction was initiated by addition of APS (11.41 mg, 0.05 mmol) and TEMED (11.62 mg, 0.1 mmol) to the cooled solution. The reaction was allowed to proceed at 8 °C under 500 rpm stirring overnight. After 23 hours the reaction was stopped by opening the flask and exposing the solution to air. The solution was purified by dialyzing against deionized water. Approximately half of the purified product was isolated from the water by freeze-drying to calculate the yield and to achieve some dry product for future analyses. The yield of the product was 386 mg (83 %).

8.3. Synthesis of poly(methacrylic acid-co-N-acryloyl glycinamide) microgels

The same synthesis method was used in the syntheses of poly(methacrylic acid-co-N-acryloyl glycinamide) (P(MAA-co-NAGA)) microgels which was used in the synthesis of PNAGA microgel. The reaction conditions were tuned slightly as the temperature and the amounts of initiators were increased. Methacrylic acid has a melting point of 15 °C and it is soluble in water above the temperature of 16 °C. Hence the reaction temperatures of the syntheses were increased above the melting point but kept below the assumed VPTT's of the polymers adopted from the literature[28]. The reaction temperature was 16 °C for 10 %, 30 % and 70 % products and 25 °C for 50 % product. The amounts of initiators were increased to achieve an effective polymerization. All other reactions were allowed to proceed overnight but the 70 % gel, which required two nights to achieve high enough conversion. The volume of each copolymer reaction solution was 25 ml.

Unlike in case of PNAGA gel, where a dialysis was effective enough to purify the product, the P(MAA-co-NAGA) copolymer gels needed more purification. The NMR spectra of dialyzed copolymer gels

showed some water insoluble impurities and hence all the copolymer products were purified more by washing with methanol. The washing was performed by dispersing the dry product to methanol and stirred overnight. The mixture was sonicated for ten minutes before collecting the product by centrifuging and removing the methanol layer. Washing procedure was repeated three times to achieve a pure product. The pure product was dispersed in deionized water and collected by freeze drying. Amounts of starting materials and yields for the copolymer gels are presented in Table 1.

	NAGA	MAA	SDS	BIS	APS	TEMED
P(MAA-co-NAGA) 10%	202.34 mg, 1.58 mmol	15.59 mg, 0.18 mmol	28.98 mg, 0.10 mmol	8.11 mg, 0.05 mmol	34.41 mg, 0.15 mmol	33.75 mg, 0.29 mmol
P(MAA-co-NAGA) 30%	156.84 mg, 1.22 mmol	44.29 mg, 0.51 mmol	28.98 mg, 0.10 mmol	8.11 mg, 0.05 mmol	34.41 mg, 0.15 mmol	33.75 mg, 0.29 mmol
P(MAA-co-NAGA) 50%	112.26 mg, 0.88 mmol	75.74 mg, 0.88 mmol	28.86 mg, 0.10 mmol	8.09 mg, 0.05 mmol	35.86 mg, 0.16 mmol	34.90 mg, 0.30 mmol
P(MAA-co-NAGA) 70%	67.59 mg, 0.53 mmol	103.77 mg, 1.21 mmol	28.72 mg, 0.10 mmol	8.21 mg, 0.05 mmol	33.90 mg, 0.15 mmol	34.49 mg, 0.30 mmol

Yield	After dialysis	After methanol washes (pure product)
P(MAA-co-NAGA) 10%	203 mg (90%)	167 mg (74%)
P(MAA-co-NAGA) 30%	194 mg (93%)	144 mg (69%)
P(MAA-co-NAGA) 50%	170 mg (87%)	164 mg (84%)
P(MAA-co-NAGA) 70%	175 mg (97 %)	117 mg (65 %)

Table 1. Starting materials and yields of copolymers P(MAA-co-NAGA). The volume of each reaction solution was 25 ml.

8.4. Reaction kinetics

Reaction kinetics were followed by ^{1}H NMR measurements to determine the reactivity of the two monomers. The reactions were made in an NMR tube in D_2O and the spectra were recorded in every 20 minutes for the first reaction and in every ten minutes for the second reaction as it was noticed that the reaction proceeds quite quickly.

To follow the kinetics of P(MAA-co-NAGA) with 30 % of MAA, the following procedure was used. First NAGA (6.28 mg, 0.049 mmol), MAA (1.81 mg, 0.021 mmol), BIS (0.32 mg, 2.08 µmol) and SDS (1.15 mg, 3.99 µmol) were added to 5 ml vial and dissolved in 0.75 ml of D_2O. The solution was purged with nitrogen for fifteen minutes. An empty NMR tube, closed with a septum, was also purged. After purging, the solution was transferred from the vial to the tube. The reaction was initiated by addition of nitrogen purged APS (1.37 mg, 6.00 µmol) and TEMED (1.39 mg, 11.96 µmol) solutions so that the final volume of the reaction solution was 1 ml. The reaction was allowed to proceed overnight at 16 °C during which the reaction was followed by NMR measurements. The same procedure was used for 50 % product. The amounts are presented in Table 2.

	NAGA	MAA	SDS	BIS	APS	TEMED
P(MAA-co-NAGA) 50%	4.48 mg, 0.035 mmol	3.01 mg, 0.035 mmol	1.15 mg, 3.99 µmol	0.32 mg, 2.08 µmol	1.37 mg, 6.00 µmol	1.39 mg, 11.96 µmol

Table 2. Starting materials for the kinetics reaction of P(MAA-co-NAGA) with 50 % of MAA. The volume of the reaction solution was 1 ml.

9. Characterization

9.1. Differential scanning calorimetry (DSC)

DSC measurements were performed using TA Instrument DSC Q2000, using Tzero aluminum pans. Nitrogen flow was 50 ml/min and the heating range was from 20 °C to 170 °C with heating rate of

10 °C/min. Sample size was around 2 mg. The results were plotted and analyzed by using OriginPro software.

9.2. Visual observation

Visual observations were made with a 1 w% (10 mg/ml) polymer dispersions in D_2O. Dispersions were first observed at room temperature and then cooled to 4 °C to determine the phase transition behavior. After that, the pH of the copolymer dispersions was lowered to 3 by addition of HCl at room temperature and observations were made again at 23 °C and at 4 °C. The samples at pH 3 were also observed in 40 °C. The pH of the dispersions was determined by VWR pHenomenal IS 2100L pH-meter. The meter was calibrated with three standards prior to use.

9.3. Nuclear magnetic resonance spectroscopy (NMR)

^1H NMR measurements in varied temperatures were made by using 500 MHz Bruker Avance III spectrometer. Concentrations of the samples were 10 mg/ml and the used solvent was deuterium oxide (D_2O). Conversion samples were prepared by mixing 0.1 ml of reaction solution and 0.5 ml of D_2O. In multi temperature measurements the temperature was increased from 5 °C to 60 °C and the spectra were measured in every 5 °C. Stabilization time before measurement was 600 s. In other measurements the used temperature was 23 °C, if not mentioned otherwise. TopSpin software was used to process the data and the spectra were plotted using OriginPro software.

9.4. Microcalorimetry

Microcalorimetry measurements were made by using Malvern Microcal PEAQ-DSC. Before measurements the samples were degassed by ThermoVac Sample Degassing and Thermostat instrument from MicroCal. 1 w% dispersions in D_2O were used with the sample size of 250 µl. The temperature range was from 5 °C to 60 °C and the rate was 1 °C/min in both heating and cooling. D_2O was used as a baseline. The data were exported by using MicroCal PEAQ-DSC software and analyzed by using OriginPro software.

9.5. Dynamic light scattering (DLS)

DLS measurements were performed using Brookhaven Instrument BI-200SM goniometer, BIC-TurboCorr digital pseudo-cross-correlator and a BI-CrossCorr detector. The used light source was Sapphire 488-100 CDRH from Coherent GmbH. The laser was operated at 488 nm (blue light) 30 mW power. A pinhole of 400 µm was used and measurements were made at 90° angle. Measurements were made in three temperatures: 15 °C, 25 °C and 40 °C using LAUDA RC 6 CP thermostat to control the temperature. 1 mg/ml dispersions in deionized water at pH=3 were used. Scattering data was collected for three minutes.

A Malvern Zetasizer Nano ZS instrument was used for variable temperature DLS. 1 mg/ml dispersions in deionized water at pH=3 were used. The temperature range was from 5 °C to 70 °C. The data was exported by using Zetasizer software and processed with OriginPro software.

9.6. Turbidimetry

Transmittance of the dispersions was studied by using Jasco V-750 UV-Visible spectrophotometer with Jasco CTU-100 circulating thermostat unit. The data was collected with Spectra Manager software and exported with Spectra Analysis software. The analysis of the spectra was made with OriginPro software. The concentration of the samples were 10 mg/ml and the solvent was D_2O. The temperature range was from 5 °C to 60 °C and the rate was 1 °C/min in both heating and cooling.

10. Results and discussion

10.1. DSC measurements

10.1.1. Purity of N-acryloyl glycinamide

The purity of the synthesized NAGA was determined by DSC measurement. The result of the DSC measurement is presented in the Figure 14, where the black line presents the heat flow of the twice recrystallized NAGA. The T_m was detected to be 137.8 °C for the pure product. Earlier reported values for the melting point of NAGA are 129 °C[25], 136-136.5 °C[27] and 137-139 °C[26] but also melting points up to 143 °C[14] and 145 °C[11] are reported. As the melting temperature of the synthesized NAGA was close to 138 °C the monomer was concluded to be pure.

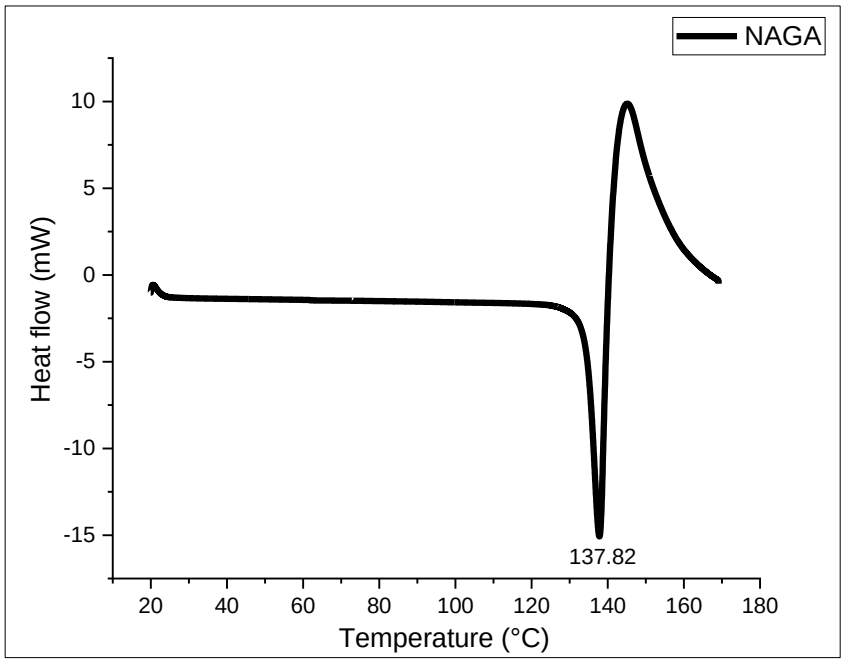

Figure 14. The heat flow curve as a function of temperature for twice recrystallized NAGA. An exothermic heat flow after melting is caused by the polymerization of the monomer.

10.2. Visual observation of the prepared microgels

1 w% PNAGA dispersion in D_2O was observed at room temperature and after cooling to 4 °C. The dispersion was slightly turbid already in 23 °C but turned more turbid upon cooling, Figure 15. The pH of the PNAGA dispersion was lowered to 3 and same observations were made. The pH values are presented in Table 3. No clear difference was observed at room temperature after the addition of HCl but a huge difference was observed when the dispersion was cooled to 4 °C. The dispersion where the pH is 3 turned much more turbid than the original dispersion. This can be explained by the acrylate impurities in the NAGA monomer. When the NAGA monomer is prepared a small amount of acrylate impurities easily stay in the product. When the slightly impure monomer is polymerized the acrylic acid units can be incorporated to the polymer. These can suppress the UCST behavior. The pH of the PNAGA dispersion in D_2O was 5.4, Table 3, which also leads to the conclusion that small amount of AA units could be incorporated to the polymer. When the pH is lowered to 3 the acrylic acid units are screened and the polymer phase transition takes place more effectively.

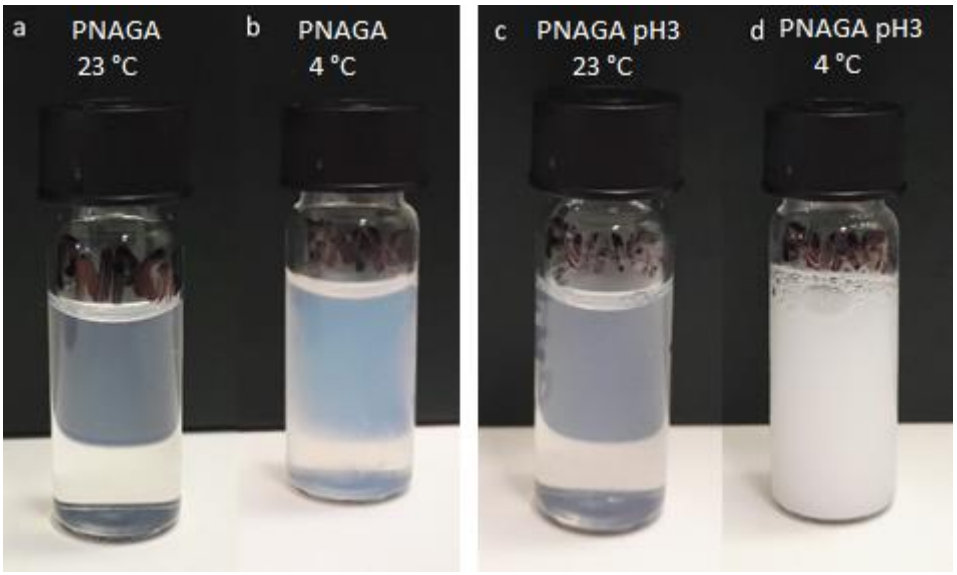

Figure 15. 1 w% PNAGA dispersion in D_2O in a) 23 °C and b) 4 °C and 1 w% PNAGA dispersion where the pH is 3 in c) 23 °C and d) 4 °C.

The 1 w% P(MAA-co-NAGA) copolymer dispersions in D_2O were observed at room temperature and after cooling to 4 °C. All dispersions apart the 70 % dispersion were clear at both temperatures, Figure 16. The P(MAA-co-NAGA) copolymer with 70 % of MAA didn't disperse in D_2O completely and the dispersion was slightly turbid through studied temperatures. The effect of MAA is clearly seen when the samples are compared to the pure PNAGA sample presented in Figure 15. The PNAGA gel dispersion is turbid in both 23 °C and in 4 °C whereas the P(MAA-co-NAGA) dispersions will not turn turbid even upon cooling. This behavior was not expected because according to literature[28] the linear MAA-NAGA copolymers can show phase transition in water also. The reason for the lack of phase transition behavior in water dispersion could probably be due to the deprotonated methacrylic acid groups from MAA, which prevent the phase transition.

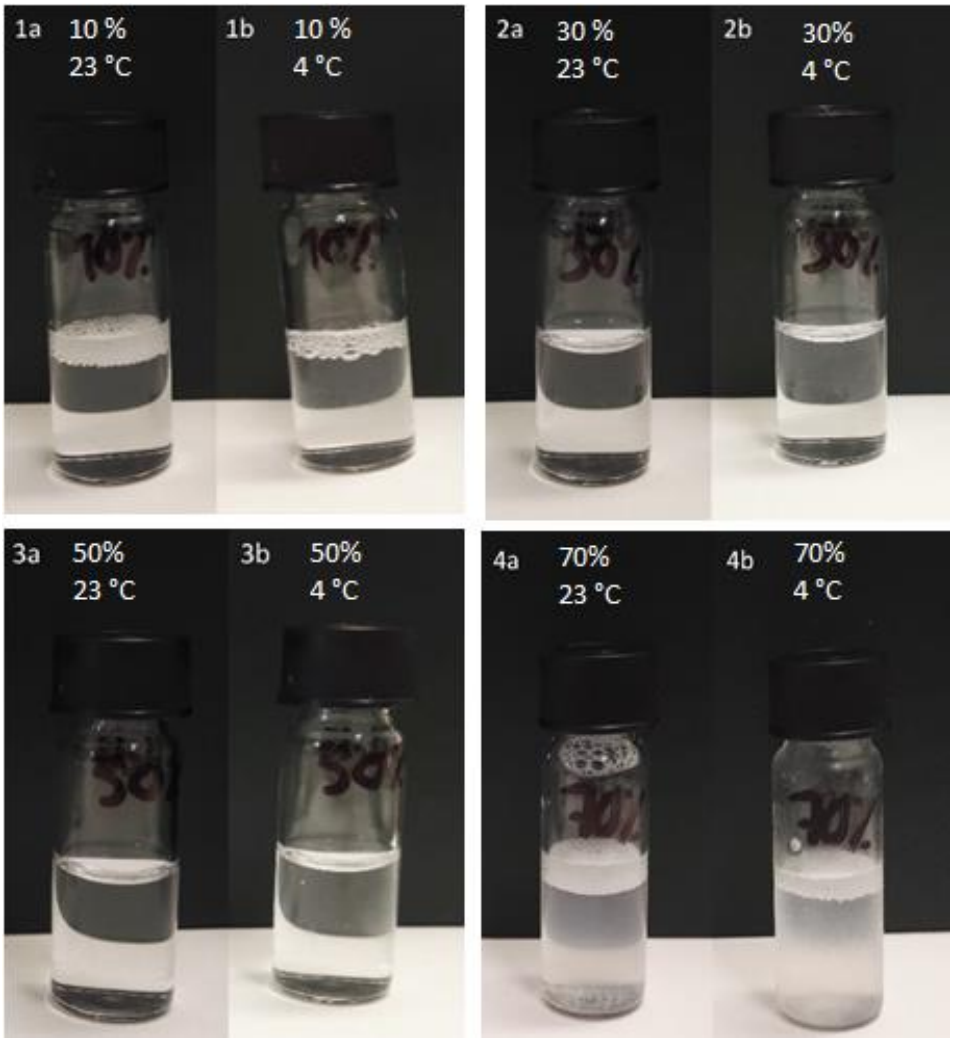

Figure 16. P(MAA-co-NAGA) 1 w% dispersions in D_2O. 1a) 10 % product in 23 °C, 1b) 10 % product in 4 °C, 2a) 30 % product in 23 °C, 2b) 30 % product in 4 °C, 3a) 50 % product in 23 °C, 3b) 50 % product in 4 °C, 4a) 70 % product in 23 °C and 4b) 70 % product in 4 °C.

The pH of the prepared 1 w% polymer dispersions in D_2O were determined before and after the addition of HCl and the results are presented in the Table 3. Before the addition of HCl all the copolymer dispersions, except the poorly dispersing 70 % dispersion, were clear at both 23 °C and 4°C, Figure 16. The lowering of the pH was done at room temperature.

Sample	Start pH	End pH
PNAGA	5.4	3.0
10 % P(MAA-co-NAGA)	4.3	3.0
30 % P(MAA-co-NAGA)	4.4	3.0
50 % P(MAA-co-NAGA)	4.5	3.0
70 % P(MAA-co-NAGA)	4.3	3.0

Table 3. pH of the 1 w% polymer dispersions before and after the addition of HCl.

Already during the addition of HCl at room temperature the 30 %, 50 % and 70 % products started to turn turbid and after reaching to pH 3, all of them were turbid. The 50 % product precipitated a little and the 70 % product precipitated strongly during the addition of HCl. The 10 % product stayed almost clear at room temperature showing only very slight turbidity. PNAGA dispersion didn't change at all. At 4 °C all the P(MAA-co-NAGA) copolymer dispersions turned turbid and all the dispersions turned clear upon heating to 40 °C, Figure 17. Only the 70 % sample had still some precipitated copolymer in the dispersion. Clearly the pH affects the phase transition behavior of the prepared copolymers, as at pH 4.5 the dispersions didn't undergo visual phase transition but at pH 3 the phase transitions were very clear in all the samples upon cooling to 4 °C and upon heating to 40 °C. Also, the bigger the amount of MAA in the copolymer the higher the phase transition temperature seem to be as the 50 % dispersion turned strongly turbid already at the room temperature, but 10 % dispersion needed the cooling to undergo the phase transition. This means that the UCST of the dispersion is increasing when the amount of MAA is increasing as was expected based on the literature[28]. The amount of MAA also affects to the dispersibility of the product as the 30 % and 50 % products dispersed to water very easily whereas the 10 % product needed more stirring and the 70 % product didn't disperse completely. Compared to the dispersibility of pure PNAGA gel, the dispersibility of 30 % and 50 % products are much better but the dispersibility of 70 % product is poorer. Due to the poor dispersibility, the 70% product was left out on further analyses as the concentration of the dispersion affects to the phase transition behavior of the polymer. As the polymer never dispersed completely, despite the repeated heating and stirring procedures, the concentration of the dispersion wasn't known, and the results wouldn't have been comparable with the other samples.

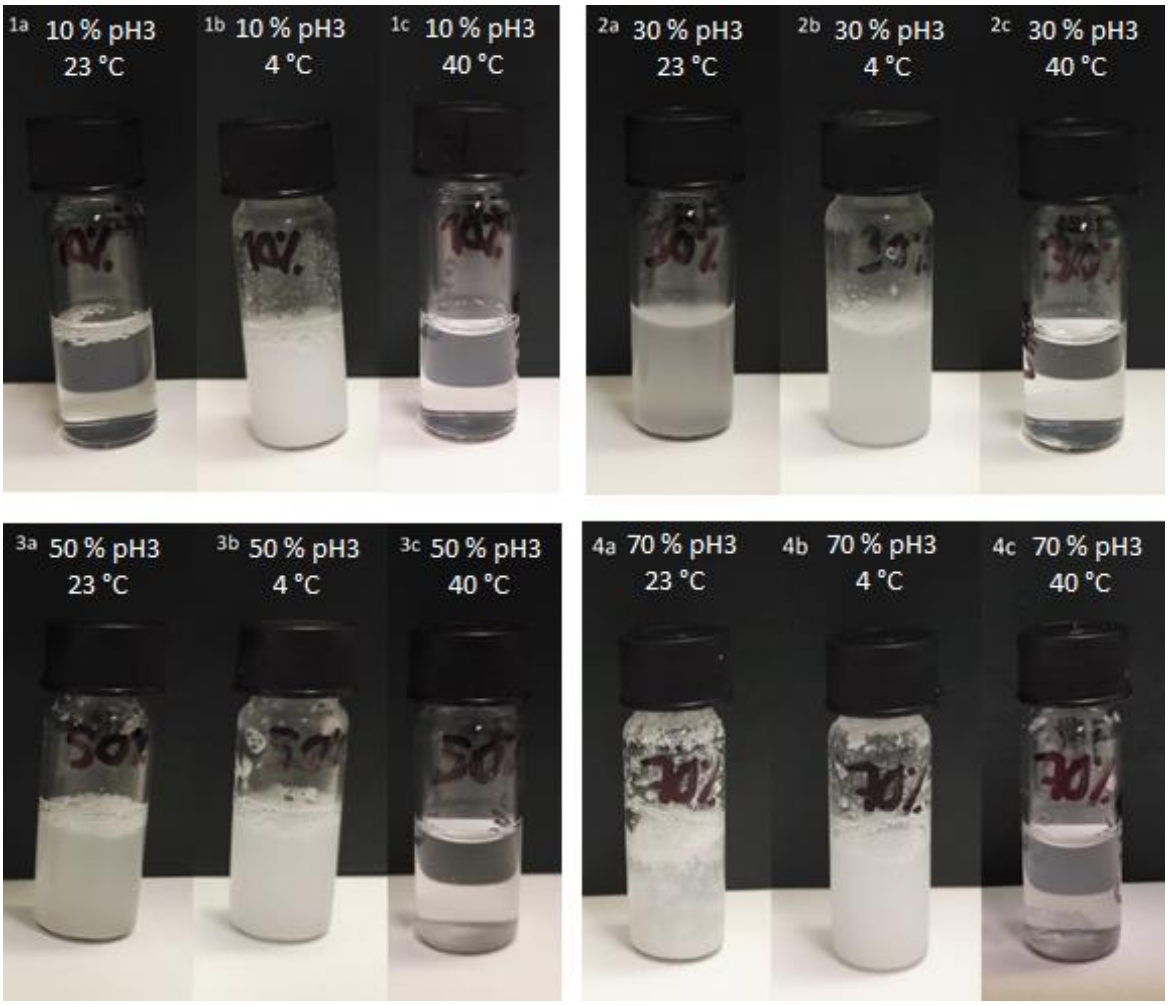

Figure 17. P(MAA-co-NAGA) 1 w% dispersions in D_2O at pH 3. 1a) 10 % product in 23 °C, 1b) 10 % product in 4 °C, 1c) 10 % product in 40 °C, 2a) 30 % product in 23 °C, 2b) 30 % product in 4 °C, 2c) 30 % product in 40 °C, 3a) 50 % product in 23 °C, 3b) 50 % product in 4 °C, 3c) 50 % product in 40 °C, 4a) 70 % product in 23 °C, 4b) 70 % product in 4 °C and 4c) 70 % product in 40 °C.

10.3. Polymerization and microgel characterization

10.3.1. Monomer conversions

The monomer conversions were determined by comparing the sample taken before initiation to the sample taken after the reaction. The conversions were calculated by comparing the monomer peaks to the D_2O peak in an NMR spectrum as the samples were prepared so that the ratio between the sample and the D_2O was kept constant. The conversions are listed in Table 4.

Sample	Conversion
PNAGA	87 %
P(MAA-co-NAGA) 10%	79 %
P(MAA-co-NAGA) 30%	83 %
P(MAA-co-NAGA) 50%	67 %
P(MAA-co-NAGA) 70%	75 %

Table 4. Monomer conversions. The conversions were calculated by comparing the monomer peaks to the D_2O peak in an NMR spectrum.

10.3.2. Reactivity ratios

NMR measurements were also made to study the reaction rates of the two monomers. The reactions were made in an NMR tube and the spectra were recorded in every ten minutes. The decrease of monomer peaks as a function of time was used to analyze the structure of the forming polymer: if both monomers have equal rate of polymerization a random copolymer can be expected. According to the literature, NAGA and MAA have similar reactivities and hence they should form statistical random copolymers.[28] Similar behavior was proved in this project as the MAA seem to react as fast as the NAGA. The reactivity of the monomers is presented in the Figure 18, where the intensities of the monomer peaks are plotted as a function of time. The intensities were detected by comparing the intensities of the monomer peaks to the intensity of D_2O peak, which doesn't change during the reaction. In the Figure 18 both original data and normalized data are presented. From the normalized data it's very easy to see that the reactivities of the monomers are very similar. Hence, statistical random copolymer can be thought to form as was expected based on the literature. It would also seem that the overall reactivity is faster in the 30% product than in the 50% product. However, clear conclusions on how the amount of MAA affects to the reaction kinetics can't be done based on only these two measurements.

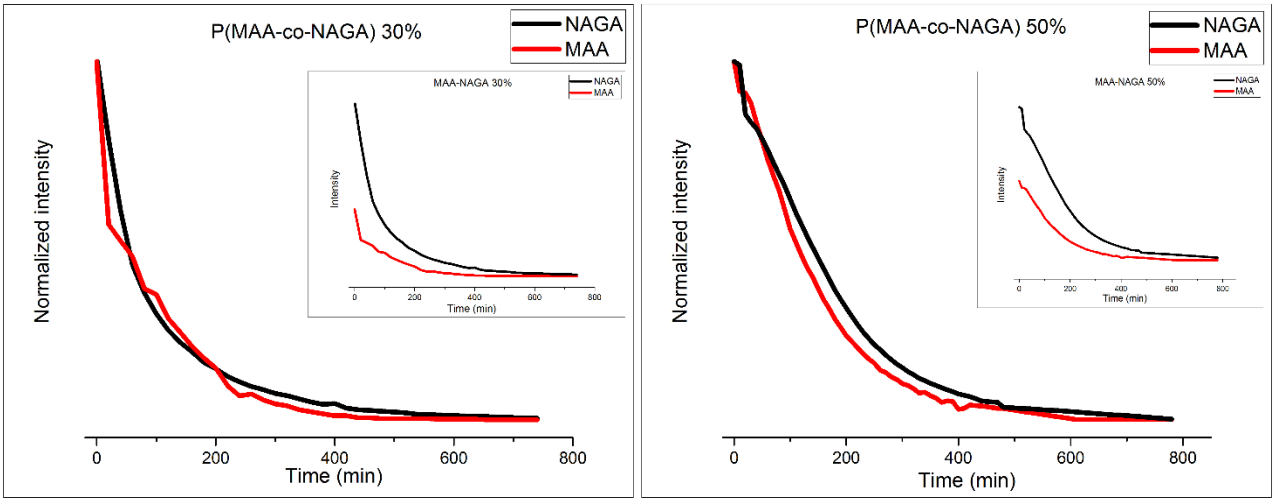

Figure 18. Reaction kinetics results for the P(MAA-co-NAGA) microgels with 30% and 50% of MAA. The intensities of the monomer peaks are presented as a function of time. Original data is stacked. Normalized intensities clearly show the similar reactivities of the two monomers.

10.3.3. PNAGA and P(MAA-co-NAGA) microgels

The structures of PNAGA and PMAA are presented in the Figure 19 with the spectra of PNAGA and P(MAA-co-NAGA). The signals coming from PNAGA and P(MAA-co-NAGA) are marked with numbers from 1 to 5. The methyl group signal from PMAA, marked with number 5, can be only found in the copolymer spectrum. The methylene group signals from polymer backbones, marked with 1 and 4, are overlapping in the copolymer spectrum. As only the signals 1 and 4 are overlapping, the analysis for example for the composition of the copolymer is easy to make, by analyzing the signals marked with 3 and 5. It also gives an opportunity to compare the possible differences in thermal behavior of the polymers in the copolymer.

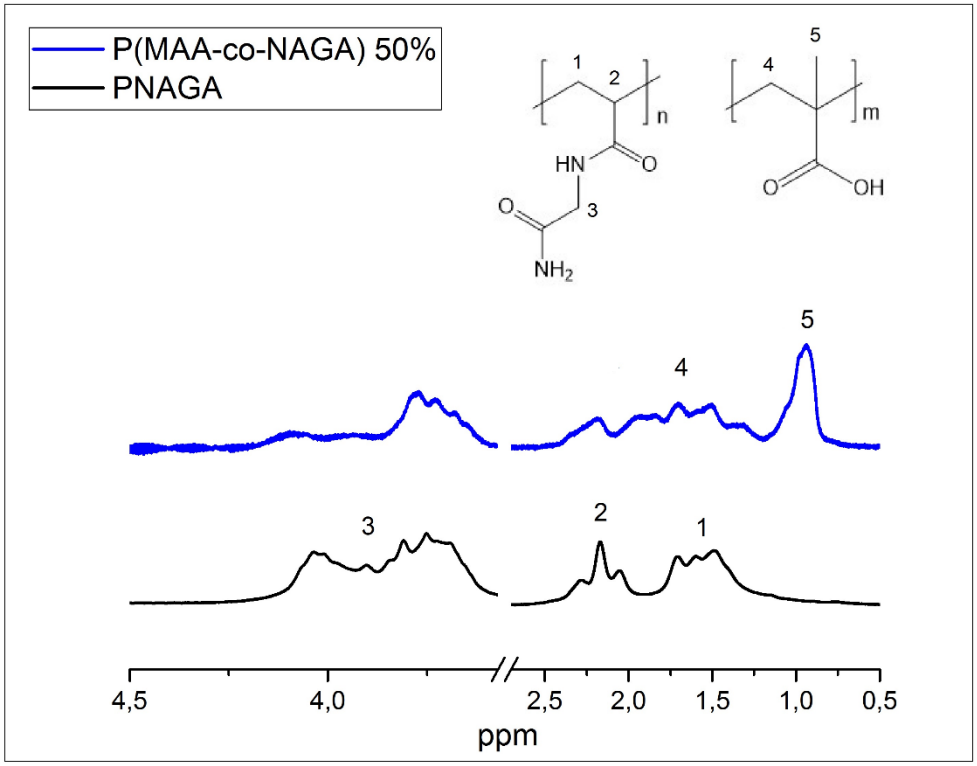

Figure 19. Structures of PNAGA and PMAA repeating units and the spectra of PNAGA and P(MAA-co-NAGA) with 50 % of MAA at 23 °C.

10.3.3.1. Composition of P(MAA-co-NAGA) microgels

The ^{1}H NMR spectra of PNAGA and all P(MAA-co-NAGA) microgels are presented in Figure 20. The MAA peak around 1 ppm appears already in 10 % sample and becomes stronger when the amount of MAA is increased. Inversely, the amount of NAGA repeating units decreases when the amount of MAA repeating units is increased in the copolymer. This is seen as a change of shape and intensities of the PNAGA peaks. Hence, from the Figure 20 it can be clearly seen that the ratio of the polymers in the copolymer are changing between samples as was wanted.

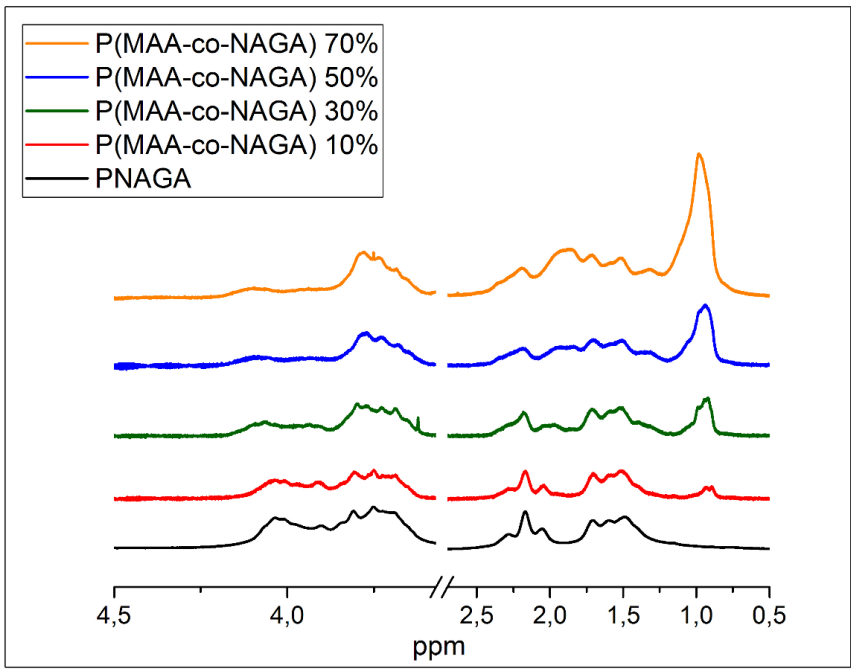

Figure 20. ^{1}H NMR spectra of PNAGA and P(MAA-co-NAGA) microgels at 23 °C. The PMAA peak, which cannot be seen in PNAGA gel, appears stronger around 1 ppm when the amount of MAA increases.

The ratio of polymers in the copolymer was determined by comparing the methylene group signal of PNAGA to the methyl group signal of PMAA in the copolymer spectrum. The integrated areas were normalized by dividing the area by the number of protons in the structure. The calculated amounts are presented in the Table 5. The ratios correlate extremely well with the amount of monomers in the feed.

Sample	Monomer ratio (MAA:NAGA)	Repeating unit ratio (MAA:NAGA)
P(MAA-co-NAGA) 10%	10:90	11:89
P(MAA-co-NAGA) 30%	29:71	30:70
P(MAA-co-NAGA) 50%	50:50	51:49
P(MAA-co-NAGA) 70%	70:30	68:32

Table 5. Monomer ratios in the feed and ratios in the copolymer gels calculated from the NMR spectra.

10.3.3.1.1. Purity of P(MAA-co-NAGA) microgels

P(MAA-co-NAGA) microgels were purified first by dialyzing against deionized water. The dialyzed products were collected by freeze drying and the dried products were analyzed by ^{1}H NMR measurements. The NMR-spectra showed some small molecular weight impurities. The impurities were determined to be small molecular weight products by DOSY measurement, which showed that the diffusion of the impurities was much faster than the diffusion of the polymer. Also, the sharpness of the impurity lines in the ^{1}H NMR spectra indicate the small size. The impure spectra of the P(MAA-co-NAGA) 10 % product and the pure PNAGA spectrum are presented in Figure 21 for comparison. The origin of the impurities was assumed to be some side reaction between some of the starting material and MAA. This was assumed because the impurities were no present in the pure PNAGA microgel, as seen from Figure 21, and because the amount of the impurities increased when the amount of MAA was increased.

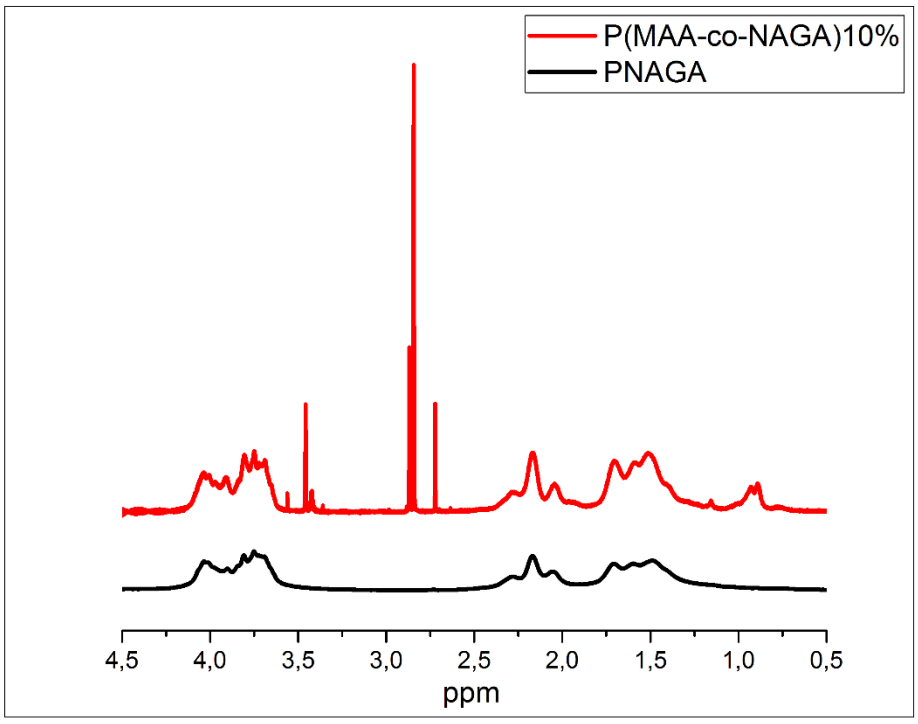

Figure 21. Spectra of P(MAA-co-NAGA) with 10 % of MAA and PNAGA gel as reference. Both spectra are recorded after dialysis. The P(MAA-co-NAGA) gels had some small molecular weight impurities which were not observed in PNAGA gel.

To remove the impurities, the samples were extensively washed with acetone, ethanol and methanol. Only the washing with methanol decreased the amount of impurities in the samples and hence all the P(MAA-co-NAGA) copolymer microgel samples were washed three times with methanol. The washing was done by mixing the product with methanol overnight followed by a heating and a ten minutes sonication and then centrifuging to collect the solid sample. After three washing cycles the products were allowed to dry and then dispersed in deionized water and collected by freeze drying. Dispersing in water and freeze drying was done because after the centrifuging and drying from methanol the product was very dense. After freeze drying the product turned back to light and fluffy as it was before the washing. The spectra for the P(MAA-co-NAGA) 10 % sample before and after the three washing cycles are presented in the Figure 22. The amount of impurities decreased significantly. However, the amount of impurities left in the product increased when the amount of MAA increased. Therefore, for example the 50 % product contained much more impurities than the 10 % product after washing cycles. This can be either due to the overall bigger amount of impurities in the sample or due some effect of MAA as it can probably bind the impurities stronger to the structure when the amount of MAA is bigger. After all, the washings were concluded to be effective enough as the amount of impurities in all the samples decreased considerably. As every washing cycle decreases the amount of the final product the amount of washing cycles was kept moderate and three was concluded to be enough.

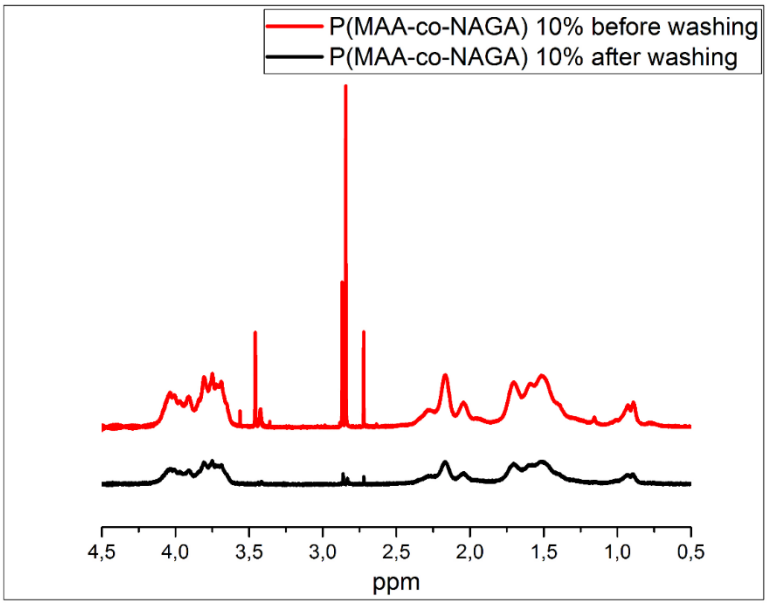

Figure 22. Spectra of P(MAA-co-NAGA) including 10 % of MAA before and after three washing cycles. The amount of impurities decreased considerably.

10.3.4. Variable temperature measurements

Multiple temperature NMR measurements were made for all the samples to follow their thermal behavior. The temperature range was from 5 °C to 60 °C and the spectra were recorded every five degrees. The multitemperature measurements were made for samples dispersed in D_2O and for D_2O with pH adjusted to 3. The spectra of PNAGA, P(MAA-co-NAGA) 10%, 30% and 50%, all in D_2O and also at pH=3, are presented in Figures 24, 25, 26 and 27, respectively. Due to poor dispersibility the 70% product was left out of these studies.

According to Figure 24 PNAGA seems to behave quite similarly in D_2O and at pH 3. This was expected as PNAGA itself shouldn't have pH sensitivity. When the temperature is 5 °C, the intensity of the signals is very weak indicating that the polymer has strong hydrogen bonding with itself and the chain mobility is collapsed. When the temperature is increased the hydrogen bonds dissociate gradually and the gel swells as seen in stronger intensity of the peaks. The intensities of the peaks are also presented as a function of temperature. The intensity vs. temperature curves are constructed so that the integrated areas of the polymer peaks are compared to the integrated area of D_2O peak in every temperature as the integral of D_2O shouldn't change as a function of temperature. NAGA repeating unit peak around 4 ppm (black circle) and MAA repeating unit peak around 1 ppm (red circle) were used to construct the intensity vs. temperature curves, Figure 23.

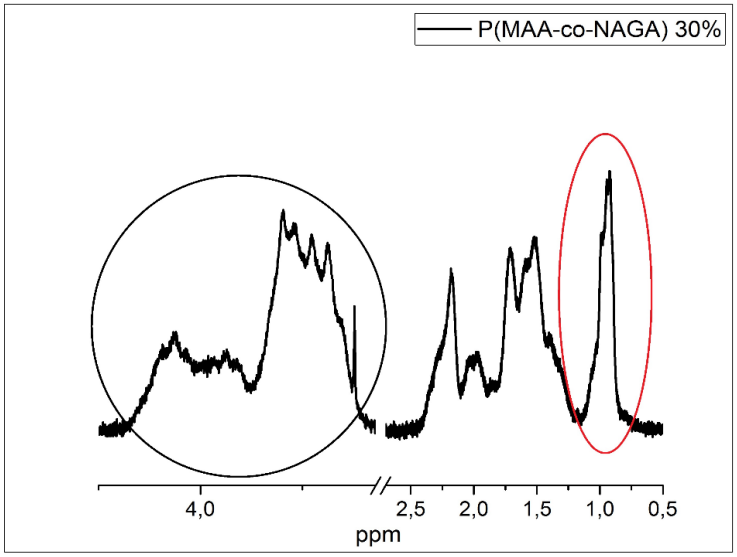

Figure 23. NAGA repeating unit peak around 4 ppm (black circle) was used to construct the intensity vs. temperature curves for PNAGA and P(MAA-co-NAGA) microgels. Similarly, MAA repeating unit peak around 1 ppm (red circle) was used to follow the intensity as a function of temperature for copolymer P(MAA-co-NAGA) microgels.

From the intensity curve of PNAGA in D_2O it can be seen that there are two areas were the intensity of the PNAGA increases faster, approximately at 15 °C and 40 °C, indicating that at these points the swelling is faster. When the pH is 3 similar faster swelling is detected at 20 °C but not so clearly in 40 °C. This indicates that there are indeed some differences between the samples in D_2O and at pH 3 as was also already seen in visual observations. The differences can be possibly explained by small acrylic acid impurities which could be from the synthesis of NAGA. Acrylic acid is strongly pH sensitive and it could explain changes in behavior of PNAGA upon the change of pH. Overall no sharp VPTT is observed in either of the samples.

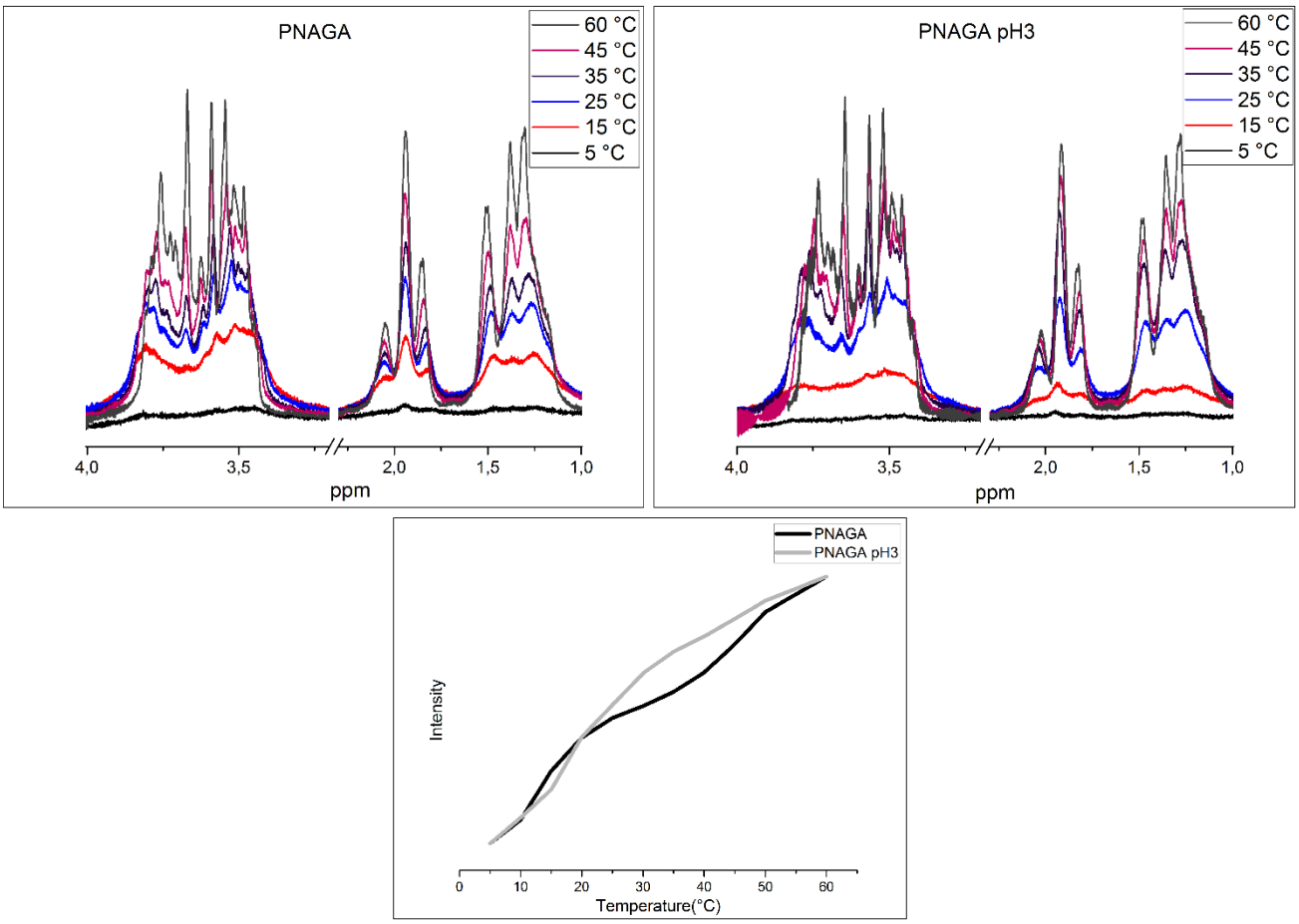

Figure 24. ^1H NMR multitemperature measurements of PNAGA in D_2O and at pH 3. The results are also presented in intensity as a function of temperature, where intensity means the integral of sample signals vs. solvent signal.

In P(MAA-co-NAGA) 10 % sample the difference is huge between D_2O and at pH 3, Figure 25. No change is seen in D_2O as the spectra are almost identical at all temperatures. This correlates nicely with the visual observations as there was no visible change. At pH 3 the change can be seen clearly as in low temperatures the intensities are very low and when the temperature is increased also the intensities increase. However, the growth of the polymer peaks ends around 30 °C which didn't happen in the case of pure PNAGA where the intensities of the peaks increased through the whole temperature range. This indicates that the MAA sharpens the thermal behavior of the polymer in the molecular level as the hydrogen bonds between the polymer break easier and the hydrogen bonds between the polymer and the water form easier. In D_2O the thermal swelling is not seen as the MAA units are deprotonated and hence the hydrogen bonds between the polymers are broken. Therefore, the polymer doesn't show changes even in molecular level.

Overall, some interesting observations can be made. First is that the signal to noise ratio of the sample in D_2O is quite different compared to the sample at pH 3. It is somehow surprising that the spectrum at pH 3 shows sharper signals than the spectrum in D_2O. Another interesting observation is that in D_2O the signals around 4 ppm shifts, but others do not. This behavior is also observed in other copolymer microgels, as is seen later in figures 26 and 27. The reasons for these behaviors are not known.

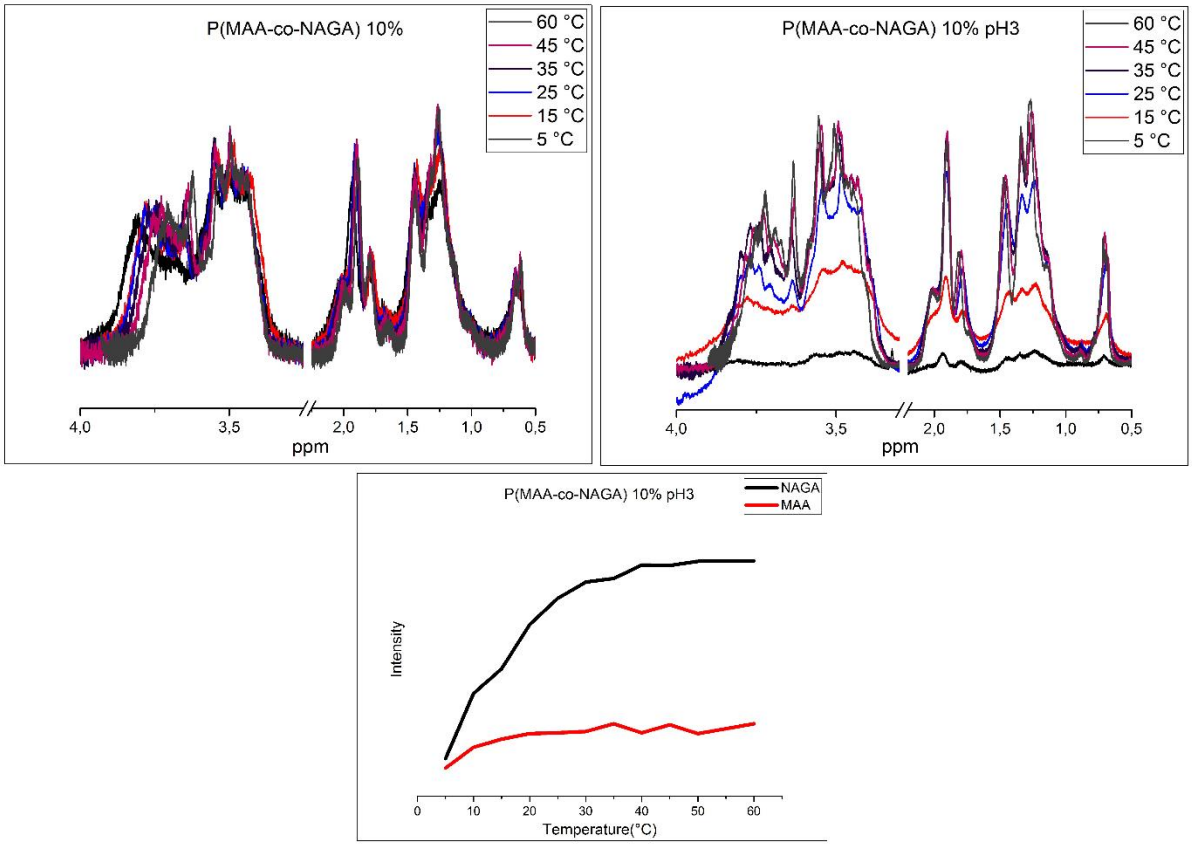

Figure 25. The ^{1}H NMR multitemperature measurements of P(MAA-co-NAGA) 10% in D_2O and at pH 3. The results at pH 3 are also presented in intensity as a function of temperature, where intensity means the integral of sample signals vs. solvent signal.

The multitemperature NMR spectra for the P(MAA-co-NAGA) 30 % product in D_2O and at pH 3 are presented in Figure 26. When compared to 10 % product the results in D_2O look very similar as there is no change in molecular level in different temperatures. At pH 3 a few differences can be noticed. The first is that already at low temperatures the molecules are more mobile than in 10 % sample or pure PNAGA sample. This is seen as a larger intensity of the peaks in low temperatures. For the pure PNAGA sample in 5 °C the movement of the polymer was completely suppressed as the polymer had so strong hydrogen bonding with itself. When the amount of MAA increases the hydrogen bonds between polymer units seem to decrease as the movement of the polymer is freer even in lowest temperatures. Also, the increase in the intensities seem to end at approximately 25 °C which also indicates looser hydrogen bonds between polymers and stronger hydrogen bonds between polymer and water.

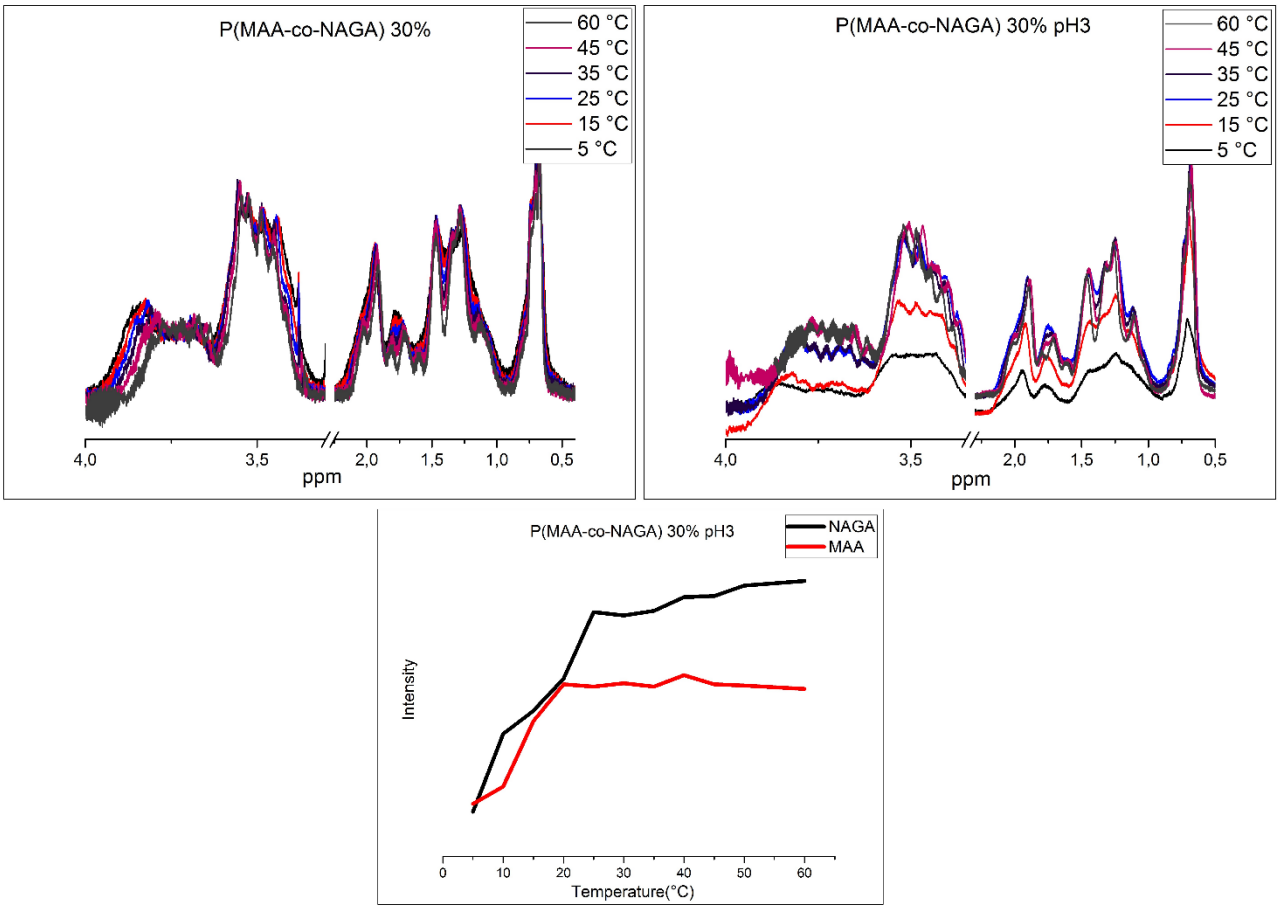

Figure 26. The ^{1}H NMR multitemperature measurements of P(MAA-co-NAGA) 30% in D_2O and at pH 3. The results at pH 3 are also presented in intensity as a function of temperature, where intensity means the integral of sample signals vs. solvent signal.

The results for the P(MAA-co-NAGA) 50 % sample go well in line with the other NMR measurements, Figure 27. There is no change in the spectra which were recorded in different temperatures for the sample in D_2O. At pH 3 the change is seen but it is much more suppressed compared to the pure PNAGA sample. The molecules seem to move quite freely already at 5 °C and no changes in intensities are observed above 25 °C. So, hydrogen bonds between polymer and water seem to increase as the amount of MAA units increase in the polymer. This enables chains to move freely at low temperatures and changes the temperature range where the change happens in molecular level. This means that increased amount of MAA sharpens the UCST behavior of the polymer which could be useful for example in release applications.

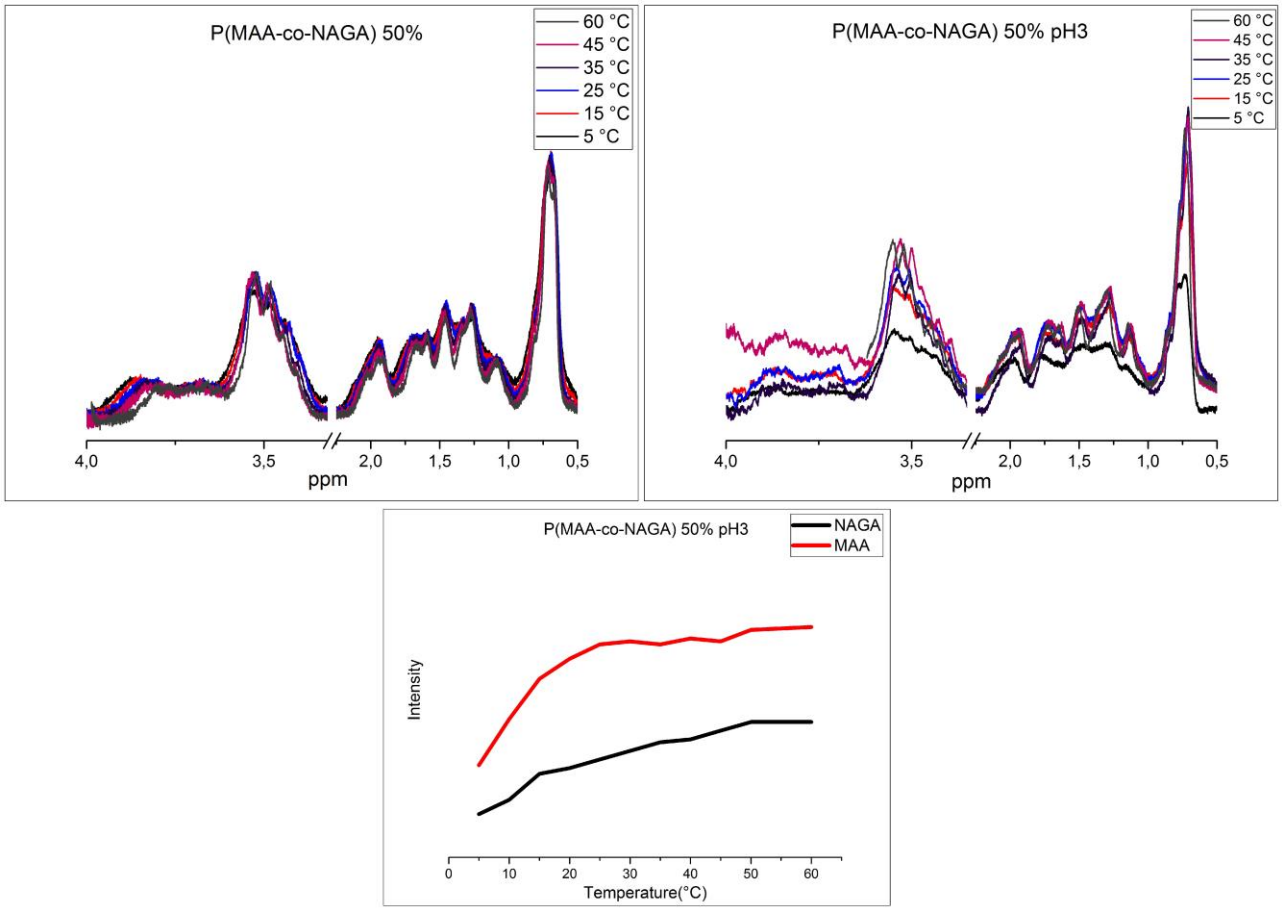

Figure 27. ^{1}H NMR multitemperature measurements of P(MAA-co-NAGA) 50% in D_2O and at pH 3. The results at pH 3 are also presented in intensity as a function of temperature, where intensity means the integral of sample signals vs. solvent signal.

10.4. Microcalorimetry

Microcalorimetry experiments were made to determine the heat flow of the samples as a function of temperature. Before adding the sample, the solvent, D_2O, was measured twice to get reliable baseline. The second cycle was used as the baseline. The results of microgel runs are presented in Figure 28. PNAGA microgel in D_2O and in pH 3 show two peaks, the first peak around 15 °C and the second around 40 °C. This indicates that the expansion of the microgel particles happen in two steps or that there are particles with different sizes and that these particles expand at different temperatures. As the crosslinker reacts faster than the monomer the crosslinker concentration is bigger in the core than in the corona causing the core to be denser than the corona. Therefore, the two-step expansion could be due to the density differences of the particles as the lower

temperature could cause the looser corona to expand but the denser core could require higher temperatures. More studies should be made to find out the exact reason for the behavior. The pH has an effect as the enthalpy is much larger at pH 3 compared to D_2O. This correlates to the visual change as it was also much bigger in pH 3. In NMR results, no big difference was observed between the PNAGA in D_2O and at pH 3, so microcalorimetry measurements and NMR measurements doesn't correlate well.

For P(MAA-co-NAGA) microgels the enthalpy is smaller compared to pure PNAGA gel. The bigger the amount of MAA in the polymer, the smaller the observed enthalpy. This is understandable as the NAGA is the thermoresponsive part in the polymer and when the amount is lowered the thermal response is smaller. In P(MAA-co-NAGA) 10% product clear peaks are seen around 15 °C and around 35 °C. These correspond quite nicely to the peaks seen for PNAGA gel. In P(MAA-co-NAGA) 30% product a small peak is detected around 15 °C and very broad peak around 30 °C. The peak around 15 °C is observed in all samples but the peak at higher temperature, around 35 °C, moves to lower temperature when the amount of MAA increases. In P(MAA-co-NAGA) 50% product only a very broad peak is detected around 25 °C. However, the peaks are so broad that no clear conclusions can be made based on them. What is clear is that the enthalpy of the transitions decreases as the amount of MAA repeating units increases in the copolymer microgels.

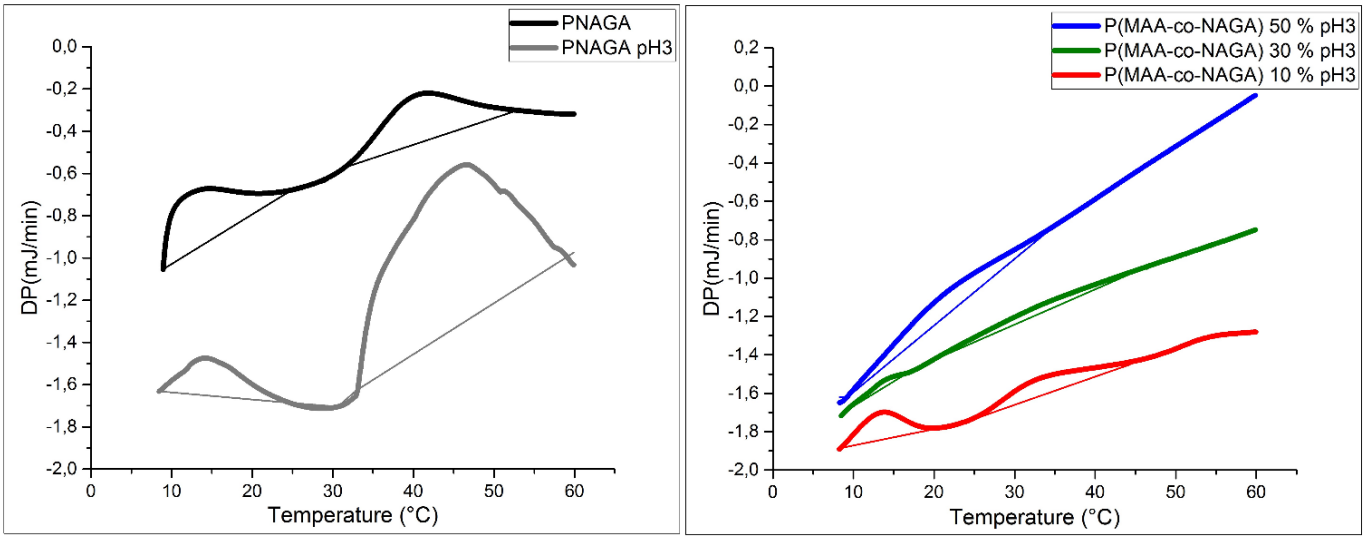

Figure 28. Heat flow of the microgels as a function of temperature. As the amount of PNAGA decreases in the product the amount of released heat decreases.

Enthalpy of the transitions were calculated by integrating the heat flow as a function of temperature curves, straight lines in Figure 28. Enthalpies were calculated using the integrated areas and known parameters of the measurements: concentration of the sample was 10 mg/ml, sample size was 250 µl of which 130 µl was measured and the heating rate was 1°C/min. Results are presented in Table 6.

Sample	Peak number	Temperature (°C)	Area (mJ)	Enthalpy (J/kg)
PNAGA	1	15	2.57	1970
	2	40	2.64	2030
PNAGA pH3	1	15	1.50	1160
	2	40	12.76	9820
P(MAA-co-NAGA) 10% pH3	1	15	0.90	690
	2	35	1.07	820
P(MAA-co-NAGA) 30% pH3	1	15	0.16	120
	2	30	0.70	540
P(MAA-co-NAGA) 50% pH3	1	25	1.81	1390

Table 6. Integration results and calculated values for enthalpy of the transitions.

10.5. Dynamic light scattering (DLS)

Dynamic light scattering was used to study the size of the microgel particles. The measurements were made at three temperatures, 15 °C, 25 °C and 40 °C to see if the size of the particles change as a function of temperature, Table 7. As can be seen from the Table 7, the size of the PNAGA microgel particles does not change when the temperature changes. This would indicate that the phase transition of the PNAGA happens at lower temperature. In P(MAA-co-NAGA) 10% and 30% samples a clear increase in size is seen between the 15 °C and 40 °C. The large size of P(MAA-co-NAGA) 50% sample indicate that the microgel particles have aggregated at low temperatures and that the aggregates partly break when temperature is increased.

Sample	Diameter in 15 °C (nm)	Diameter in 25 °C (nm)	Diameter in 40 °C (nm)
PNAGA	79	83	80
P(MAA-co-NAGA) 10%	44	50	63
P(MAA-co-NAGA) 30%	47	57	80
P(MAA-co-NAGA) 50%	404	240	116

Table 7. Diameters of the microgel particles according to DLS measurements.

Zeta sizer instrument was used to study the size of the particles as a function of temperature. The same samples were used as in DLS studies, but the temperature range was from 5 °C to 70 °C and the heating and cooling cycles were done multiple times to determine if the changes in the sizes are repeatable. It was noticed that in all cases the heating and the cooling cycles were repeatable after the first heating. As can be seen from the Figure 29 the size of the particles increases in all cases when the temperature is increased above room temperature. In PNAGA the size decreases quickly after 20 °C upon heating and the size starts to increase below 10 °C upon cooling. This indicates that the particles aggregate at low temperatures and that energy is needed to break the aggregates during the heating whereas during the cooling the particles seem to be stable and aggregate only at the lowest temperatures. The dynamic light scattering results do not correlate with those measured with the zeta sizer, as according to DLS the particles are much bigger and no clear increase in size is seen. The reason for the difference is not clear. In the P(MAA-co-NAGA) 10% sample a clear increase in size is seen during the heating and clear decrease in size during cooling. The change is also very similar in both directions. The results go in line with both instruments. No aggregation is seen at low temperatures which indicates that the particles should be quite stable. The P(MAA-co-NAGA) 30 % results show increase in size upon heating and decrease in size upon cooling. The change seems quite similar in both directions. The trend is similar with the DLS results but according to DLS the particles should be much smaller. Hence, these results shouldn't be completely trusted. In the P(MAA-co-NAGA) 50 % sample the behavior is different upon heating as the size first strongly decrease up to 40 °C and then starts to increase. Similar behavior is seen upon cooling but here the turning point is at 25 °C. This could indicate that the particles are aggregated at low temperatures and that the aggregates slowly break up to 40 °C which causes the decrease in the size. After the disaggregation the particles continue swelling which is seen as the increase in size. This behavior is supported by the DLS results which go well in line with the zeta sizer results. In this case also the

derived count rate, representing the scattering intensity, are presented. As can be seen, the derived count rate is large at low temperatures and decreases when temperature is increased. This suggests that the aggregates, which scatter strongly, disaggregate to looser particles upon heating. Similar diverse behavior is also seen upon cooling. These support the theory of aggregation and swelling. The increasing trend in size as a function of temperature indicates that the particles truly respond to the changes of temperature and hence behave as was expected and wanted.

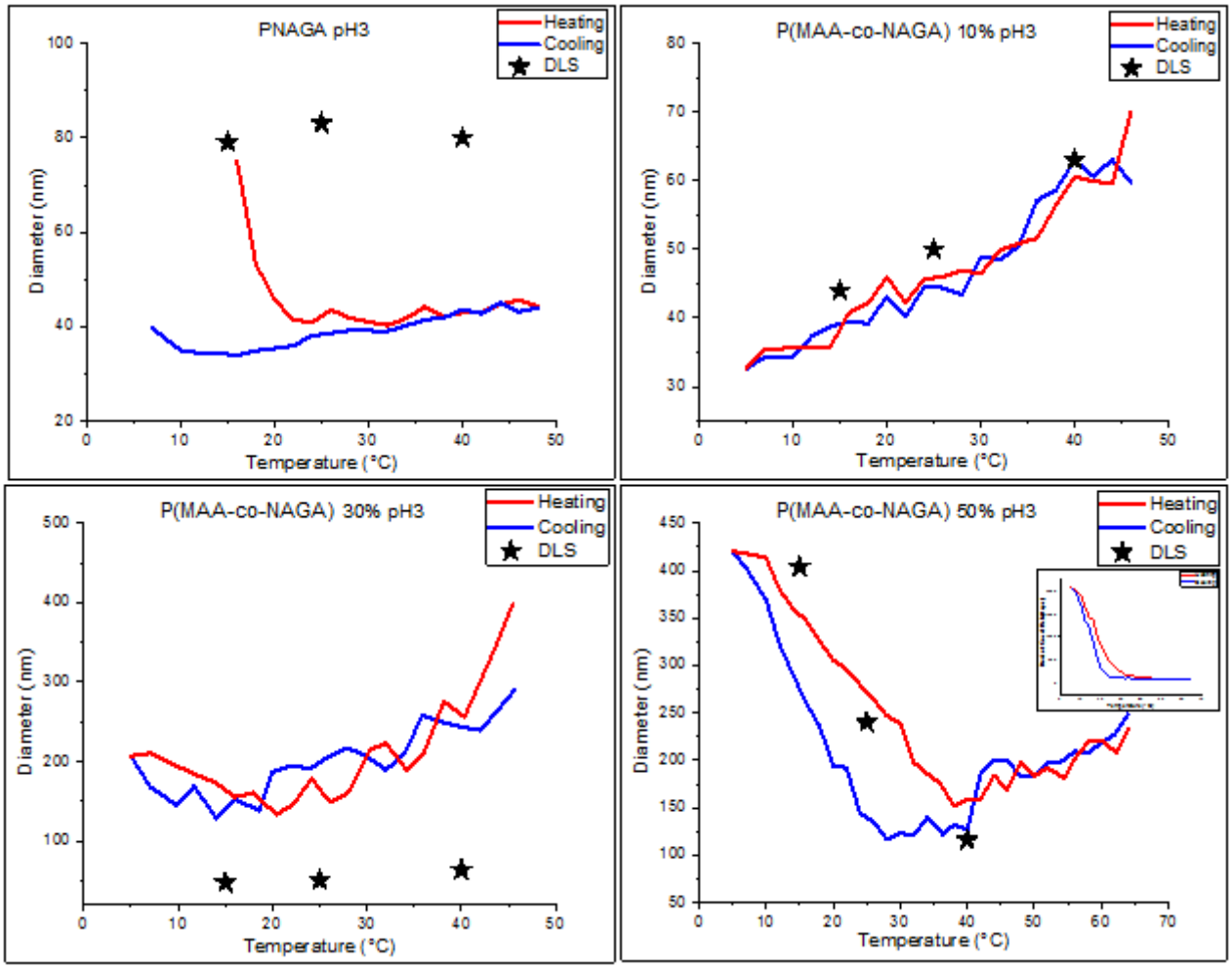

Figure 29. The diameter of the microgel particles as a function of temperature upon heating and cooling according to zeta sizer. Also, DLS results are presented in the figures. In P(MAA-co-NAGA) 50 % sample also the derived count rate is presented. The increase in size as upon heating is seen for all the microgels.

10.6. Turbidimetry

Transmittance measurements were made to determine the temperature where the dispersion changes from turbid to clear. The turbidity data are presented in Figure 30 and Table 8.

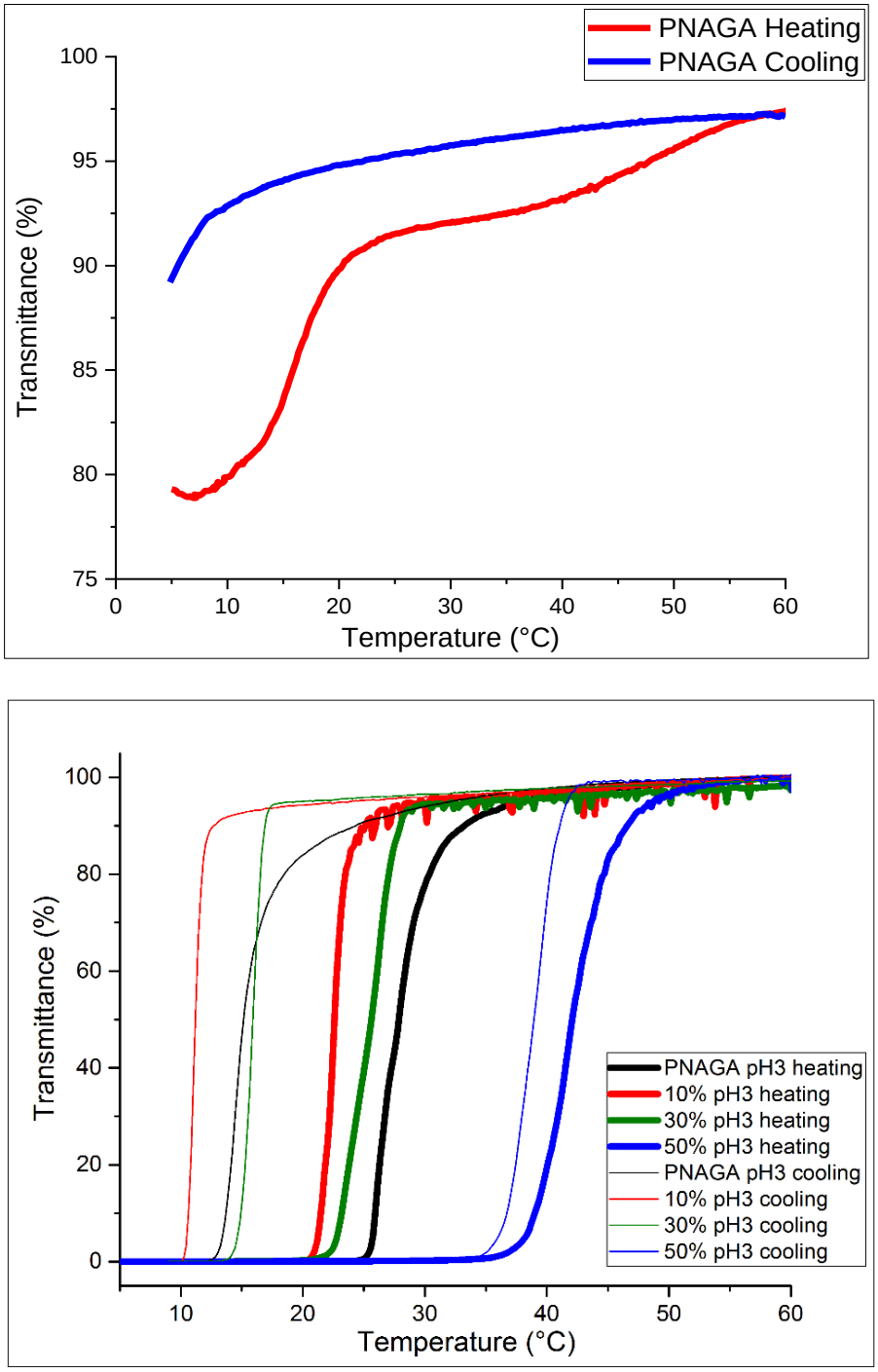

Figure 30. Transmittances of the dispersions as a function of temperature for PNAGA and P(MAA-co-NAGA) in D_2O and at pH 3.

Sample	PNAGA	PNAGA pH3	10 % pH3	30 % pH3	50% pH3
Heating	16°C / 47 °C	27 °C	22 °C	25 °C	42 °C
Cooling	7 °C	15 °C	11 °C	16 °C	38 °C
Hysteresis	9 °C	12 °C	11 °C	9 °C	4 °C

Table 8. The clearing and clouding points and the hysteresis of the microgels according to turbidimetry measurements.

For PNAGA in D_2O at 5 °C the transmittance is around 80 % and the transmittance increases in two parts when temperature is increased, Figure 30. The first quicker increase is around 15 °C and the second is around 45 °C. The transmittance goes almost up to 100 % at 60 °C. These results correlate nicely with multitemperature NMR results and with microDSC measurements where similar changes were detected. The cooling curve shows only one sharper decrease in transmittance at 10 °C. During the cooling, the temperature doesn't go low enough so that the transition would be complete.

The dispersions at pH 3 are presented in Figure 30. All the samples show very sharp transmittance change in both heating and cooling and all the samples go from 0 % transmittance to 100 % transmittance. PNAGA pH 3 has a clearing point in 27 °C upon heating and a clouding point in 15 °C upon cooling. The P(MAA-co-NAGA) 10 % sample has a clearing point in 22 °C upon heating and a clouding point in 11 °C upon cooling. In P(MAA-co-NAGA) 30 % sample these temperatures are 25 °C upon heating and 16 °C upon cooling. The P(MAA-co-NAGA) 50 % sample differs from others with significantly higher temperatures. The clearing point upon heating is in 42 °C and the clouding point upon cooling is 38 °C. From these results it can be seen that the phase transition temperature increases in the copolymer samples when the amount of MAA units increase in the polymer. Also, when the amount of MAA increases the hysteresis seem to decrease. What was unexpected was that the clearing point of the PNAGA microgel was higher than the clearing points of P(MAA-co-NAGA) microgels with 10 % and 30 % of MAA. However, this could be explained by the bigger size of the PNAGA microgels compared to P(MAA-co-NAGA) microgels with 10 % and 30 % of MAA, determined in the DLS studies. Overall the turbidity results correlate quite nicely with the earlier results. For example, in the multiple temperature NMR measurements 25 °C was the temperature where the increase in the intensities ended for the 10 % and 30 % products. In 50 % product the

turbidity results correlate with the zeta sizer results where 40 °C was the turning point where the size of the particles started to increase which was concluded to be because of the aggregation of the particles in low temperatures. The aggregation of the particles could also be one reason for the high clearing point of the dispersion in turbidity measurements, as first the aggregates must break and then the particles can swell. Also, DLS results show that the size of the particles is much bigger than the other particles, which could be an explanation for the high clearing point temperature.

What should be kept in mind is that the turbidimetry only focuses on the visual change whereas for example the microDSC and NMR focus on the changes in molecular level. This can explain the differences in the results, where the phase transition temperature would seem to be higher in molecular level than in visually observable level. For example, in the case of PNAGA in pH3 the multiple temperature NMR shows change in whole temperature range from 5 °C to 60 °C and no clear VPTT is observed. However, in turbidimetry a clear VPTT is observed at 27 °C. This is understandable as the change doesn't have to be "complete" in molecular level so that the visual observation can be made. So, when the temperature is increased the particles start to swell. At 27 °C the hydrogen bonds between polymer and water overcome the hydrogen bonds between polymers and the particles disperse in water. After that the particles continue swelling which is seen in molecular level but not anymore visually. This explains why transition temperatures according to molecular level studies can give higher phase transition values than the visual measurements and why the different methods are not directly comparable with each other.

11. Conclusions

In this work thermoresponsive microgels with different ratio of NAGA and MAA monomers were successfully prepared by surfactant stabilized free radical precipitation polymerization in presence of BIS cross linker. PNAGA microgel was synthesized as reference. D_2O dispersions were used in characterization. It was observed, that PNAGA microgel behaves differently in D_2O and at pH 3. In D_2O, the turbidity of the dispersion increased only slightly at low temperatures, as transmittance decreased to 80 %. Transmittance increased up to 100 % at two temperatures, 15 °C and 40 °C, upon heating. At pH 3, the transmittance of the dispersion decreased from 100 % to 0 % at 15 °C upon cooling and increased from 0 % to 100 % at 27 °C upon heating. So, at pH 3 the visual change was very sharp and strong whereas in D_2O the visual change was very small and the transmittance

increased gradually at two temperatures. It was concluded that small acrylic acid impurities from the monomer synthesis prevented the full phase transition behavior in D_2O. At pH 3 the acrylic acid groups are protonated enabling phase transition behavior. The different behavior of PNAGA in D_2O and at pH 3 was also observed in microcalorimetry measurements, where the enthalpy was much larger at pH 3 compared to D_2O. According to microcalorimetry, the expansion of PNAGA happens in two steps, approximately at 15 °C and 40 °C, both in D_2O and at pH 3. This result correlates well with the transmittance and multitemperature NMR results of PNAGA in D_2O, were similar two-step expansions were observed. At pH 3, multitemperature NMR didn't show clear two-step expansion as the gel expanded more stable over the whole temperature range, showing slightly faster swelling around 20 °C. Dynamic light scattering was used to measure the size of the particles and to study their thermal behavior. PNAGA microgel particles had a diameter of approximately 80 nm and the size increased and decreased when temperature was increased and decreased, respectively.

To study the effect of incorporation of MAA, P(MAA-co-NAGA) microgels with 10 %, 30 %, 50 % and 70 % of MAA were prepared. The products were studied in D_2O. It was noticed that all the products were strongly pH dependent and no phase transition behavior was observed in D_2O because of the deprotonated methacrylic acid groups. At pH 3, all samples showed phase transition behavior and hence, all measurements were made at pH 3. The P(MAA-co-NAGA) microgel with 70 % of MAA at pH 3 turned out to be very poorly dispersible and hence it was not studied thoroughly in this project. P(MAA-co-NAGA) 10 %, 30 % and 50 % products showed sharp visual phase transition upon heating and cooling. The clearing point of the product increased and the hysteresis between the heating and cooling decreased when the amount of MAA increased. Hence, according to turbidimetry, the incorporation of MAA changed the VPTT of the microgels and sharpened the phase behavior. Similar results were got from multitemperature NMR measurements as the mobility of the polymer chain increased already at low temperatures and the expansion of the microgels ended at lower temperatures when the amount of MAA increased. Microcalorimetry results showed that the enthalpy of the transitions decrease as the amount of MAA increases. This was understandable as the PNAGA is the thermoresponsive polymer. DLS measurements showed diameters of 50 nm, 60 nm and 200 nm at 25 °C for 10 %, 30 % and 50 % products, respectively. It was concluded that the 50 % product most probably aggregated at low temperatures, which caused the bigger size. Sizes of all samples increased and decreased when temperature was increased and decreased, respectively.

Overall, P(MAA-co-NAGA) microgel particles showed interesting properties as their phase transition was narrower than in case of the homopolymer microgel. Also, the UCST of the copolymer gel could be increased by increasing the amount of MAA in the product. Hence, the properties of the gels could be tuned by adjusting the monomer ratio of the copolymers.

12. Further work

Many interesting aspects was still left to study in the future. For example, some small molecular weight impurity was noticed to appear during the synthesis of copolymer microgels which didn't appear in PNAGA microgel. Washing with methanol decreased the amount of impurity but it was not able to be washed out completely. The origin or the nature of the impurity was not solved during this project. However, in the future studies, the origin of the impurity would be good to study. Then, the reaction could be modified to prevent the formation of it.

The project left also other interesting questions still to be examined. It has been said in the literature that only a limited amount of MAA can be incorporated into the copolymer to maintain successful precipitation. Loose particles, or even no particle formation, can be observed if the amount of hydrophilic substance is too big.[47] In this thesis, all the products were assumed to be microgels with similar structure. Hence in the future, it would be interesting to study the shape of the particles to found out if this indeed is the case. If the different products do not have similar crosslinked structure the products might have different properties and hence the products wouldn't be directly comparable. So, more precise analysis of the structure is needed.

Another interesting point in the synthesis is that during the work it was found out that in neutral pH the deprotonated acid groups prevent the phase behavior of the microgels. As the synthesis was done in neutral pH one could question if the synthesis method even was a precipitation polymerization in the case of copolymer microgels. It would be interesting to study if the reaction pH actually affects to the particles final form and, hence, if particles synthesized for example in acidic conditions would lead to a different product compared to what was got in this work.

It would be also interesting to study the microgel particles at different pH values. The particles were studied in D_2O, where the pH was 5.4 for PNAGA and around 4.4 for copolymer microgels (see Table 3), and at pH 3. In future studies it would be also interesting to study the properties in very acidic conditions, as at pH 1, and possibly also in very basic conditions, as at pH 9, to determine how the

behavior changes. In very acidic conditions the UCST temperature would probably be even higher than at pH 3, as all the acid groups would be fully protonated. It is indeed possible, that some of the acidic groups would still stay deprotonated at pH 3, even it is assumable that most of them are protonated as the pKa value of PMAA is 4.7[31]. In basic conditions, it is assumable that no phase behavior would be detected as wasn't even at neutral pH, due to the complete deprotonation of acid groups. This would, however, be interesting to prove.

What would be also interesting to study is the loading and release properties of the particles. According to literature, PNAGA microgels can be used as nanocatalyst platforms.[8] Hence, it would be interesting to compare the loading and release properties of formed particles and to study if the MAA increases the particles potential to be used in catalyst applications. If P(MAA-co-NAGA) microgels would seem a potential choice for catalyst platforms, it would be also interesting to determine the best ratio of the monomer units in the copolymer. By this, the particles could be tuned for needed applications.

12. References

1. Seuring J, Agarwal S. Polymers with upper critical solution temperature in aqueous solution. *Macromol Rapid Commun*. 2012;33(22):1898-1920.

2. Kean ZS, Niu Z, Hewage GB, Rheingold AL, Craig SL. Stress-responsive polymers containing cyclobutane core mechanophores: Reactivity and mechanistic insights. *J Am Chem Soc*. 2013;135(36):13598-13604.

3. Anamica, Pande PP. An overview on smart pH responsive polymers. *Asian J Chem*. 2018;30(4):711-718.

4. Ohno K, Sakaue M, Mori C. Magnetically responsive assemblies of polymer-brush-decorated nanoparticle clusters that exhibit structural color. *Langmuir*. 2018;34(32):9532-9539.

5. Pantuso E, De Filpo G, Nicoletta FP. Light-responsive polymer membranes. *Advanced Optical Materials*. 2019;0(0):1900252.

6. Aseyev V, Tenhu H, Winnik FM. Non-ionic thermoresponsive polymers in water. In: Müller AHE, Borisov O, eds. *Self organized nanostructures of amphiphilic block copolymers II.* Berlin, Heidelberg: Springer Berlin Heidelberg; 2011:29-89.

7. Alexander C, Shakesheff K . Responsive polymers at the biology/materials science interface. *Adv Mater*. 2006;18(24):3321-3328.

8. Yang D, Viitasuo M, Pooch F, Tenhu H, Hietala S. Poly(N-acryloylglycinamide) microgels as nanocatalyst platform. *Polym Chem*. 2018;9(4):517-524.

9. Smeets NMB, Hoare T. Designing responsive microgels for drug delivery applications. *J Polym Sci Part A: Polym Chem*. 2013;51(14):3027-3043.

10. Li J, Stachowski M, Zhang Z. 11 - application of responsive polymers in implantable medical devices and biosensors. *Switchable and Responsive Surfaces and Materials for Biomedical Applications*. 2015:259-298.

11. Boustta M, Colombo P, Lenglet S, Poujol S, Vert M. Versatile UCST-based thermoresponsive hydrogels for loco-regional sustained drug delivery. *Journal of Controlled Release*. 2014;174:1-6.

12. Muthiah P, Hoppe SM, Boyle TJ, Sigmund W. Thermally tunable surface wettability of electrospun fiber mats: Polystyrene/poly(N-isopropylacrylamide) blended versus crosslinked poly(N-isopropylacrylamide)-co-(methacrylic acid)]. *Macromol Rapid Commun*. 2011;32(21):1716-1721.

13. Tang Y, Wu T, Hu B, et al. Synthesis of thermo- and pH-responsive ag nanoparticle-embedded hybrid microgels and their catalytic activity in methylene blue reduction. *Mater Chem Phys*. 2015;149-150:460-466.

14. Seuring J, Bayer FM, Huber K, Agarwal S. Upper critical solution temperature of poly(N-acryloyl glycinamide) in water: A concealed property. *Macromolecules*. 2012;45(1):374-384.

15. Hashizume J, Teramoto A, Fujita H. Phase equilibrium study of the ternary system composed of two monodisperse polystyrenes and cyclohexane. *J Polym Sci Polym Phys Ed*. 1981;19(9):1405-1422.

16. Rebelo LPN, De Sousa HC, Van Hook WA. Hypercritically enhanced distortion of a phase diagram: The (polystyrene + acetaldehyde) system. *J Polym Sci B Polym Phys*. 1997;35(4):631-637.

17. Arnauts J, De Cooman R, Vandeweerdt P, Koningsveld R, Berghmans H. Calorimetric analysis of liquid—liquid phase separation. *Thermochimica Acta*. 1994;238:1-16.

18. Okada Y, Tanaka F. Cooperative hydration, chain collapse, and flat LCST behavior in aqueous poly(N-isopropylacrylamide) solutions. *Macromolecules*. 2005;38(10):4465-4471.

19. Malcolm GN, Rowlinson JS. The thermodynamic properties of aqueous solutions of polyethylene glycol, polypropylene glycol and dioxane. *Trans Faraday Soc*. 1957;53(0):921-931.

20. Halperin A, Kröger M, Winnik FM. Poly(N-isopropylacrylamide) phase diagrams: Fifty years of research. *Angew Chem Int Ed*. 2015;54(51):15342-15367.

21. Sprecht EH, Neuman A, Neher HT. US pat. 2,773,063. *Rohm & Haas*. 1956.

22. Heskins M, Guillet JE. Solution properties of poly(N-isopropylacrylamide). *J Macromol Sci A*. 1968;2(8):1441-1455.

23. Seuring J, Agarwal S. Polymers with upper critical solution temperature in aqueous solution: Unexpected properties from known building blocks. *ACS Macro Lett*. 2013;2(7):597-600.

24. Seuring J, Agarwal S. First example of a universal and cost-effective approach: Polymers with tunable upper critical solution temperature in water and electrolyte solution. *Macromolecules*. 2012;45(9):3910-3918.

25. Haas HC, Schuler NW. Thermally reversible homopolymer gel systems. *J Polym Sci B Polym Lett*. 1964;2(12):1095-1096.

26. Mäkinen L, Varadharajan D, Tenhu H, Hietala S. Triple hydrophilic UCST–LCST block copolymers. *Macromolecules*. 2016;49(3):986-993.

27. Heilmann SM, Smith II HK. Acrylic-functional aminocarboxylic acids and derivatives as components of pressure-sensitive adhesives. *J Appl Polym Sci*. 1979;24(6):1551-1564.

28. Sun W, An Z, Wu P. Hydrogen bonding reinforcement as a strategy to improve upper critical solution temperature of poly(N-acryloylglycinamide-co-methacrylic acid). *Polym Chem*. 2018;9(26):3667-3673.

29. Käfer F, Lerch A, Agarwal S. Tunable, concentration-independent, sharp, hysteresis-free UCST phase transition from poly(N-acryloyl glycinamide-acrylonitrile) system. *J Polym Sci Part A: Polym Chem*. 2017;55(2):274-279.

30. Shang L, Dong S. Facile preparation of water-soluble fluorescent silver nanoclusters using a polyelectrolyte template. *Chem Commun*. 2008(9):1088-1090.

31. Dempsey B, Serjeant EP. *Ionisation constants of organic acids in aqueous solution.* Oxford; New York: Pergamon Press; 1979.

32. Klinger D, Landfester K. Stimuli-responsive microgels for the loading and release of functional compounds: Fundamental concepts and applications. *Polymer*. 2012;53(23):5209-5231.

33. Pich A, Richtering W. Microgels by precipitation polymerization: Synthesis, characterization, and functionalization. In: Pich A, Richtering W, eds. *Chemical design of responsive microgels.* Berlin, Heidelberg: Springer Berlin Heidelberg; 2011:1-37.

34. Pelton R. Temperature-sensitive aqueous microgels. *Adv Colloid Interface Sci*. 2000;85(1):1-33.

35. Carothers WH. Polymerization. *Chem Rev (Washington, DC, U S)*. 1931;8:353-426.

36. Hennink WE, van Nostrum CF. Novel crosslinking methods to design hydrogels. *Adv Drug Deliv Rev*. 2012;64:223-236.

37. Wu X, Pelton RH, Hamielec AE, Woods DR, McPhee W. The kinetics of poly(N-isopropylacrylamide) microgel latex formation. *Colloid Polym Sci*. 1994;272(4):467-77.

38. Stieger M, Richtering W, Pedersen JS, Lindner P. Small-angle neutron scattering study of structural changes in temperature sensitive microgel colloids. *J Chem Phys*. 2004;120(13):6197-6206.

39. Virtanen OLJ, Mourran A, Pinard PT, Richtering W. Persulfate initiated ultra-low cross-linked poly(N-isopropylacrylamide) microgels possess an unusual inverted cross-linking structure. *Soft Matter*. 2016;12(17):3919-3928.

40. Virtanen OLJ, Ala-Mutka H, Richtering W. Can the reaction mechanism of radical solution polymerization explain the microgel final particle volume in precipitation polymerization of N-isopropylacrylamide? *Macromol Chem Phys*. 2015;216(13):1431-1440.

41. Gao J, Frisken BJ. Cross-linker-free N-isopropylacrylamide gel nanospheres. *Langmuir*. 2003;19(13):5212-5216.

42. Hu X, Tong Z, Lyon LA. Control of poly(N-isopropylacrylamide) microgel network structure by precipitation polymerization near the lower critical solution temperature. *Langmuir*. 2011;27(7):4142-4148.

43. Cleland RE, Grace SC. Voltammetric detection of superoxide production by photosystem II. *FEBS Lett*. 1999;457(3):348-352.

44. McPhee W, Tam KC, Pelton R. Poly(N-isopropylacrylamide) latices prepared with sodium dodecyl sulfate. *J Colloid Interf Sci*. 1993;156(1):24-30.

45. Strachota B, Matějka L, Zhigunov A, et al. Poly(N-isopropylacrylamide)–clay based hydrogels controlled by the initiating conditions: Evolution of structure and gel formation. *Soft Matter*. 2015;11(48):9291-9306.

46. Zhang S, Shi Z, Xu H, Ma X, Yin J, Tian M. Revisiting the mechanism of redox-polymerization to build the hydrogel with excellent properties using a novel initiator. *Soft Matter*. 2016;12(9):2575-2582.

47. Nayak S, Lyon LA. Soft nanotechnology with soft nanoparticles. *Angew Chem Int E*. 2005;44(47):7686-7708.

48. Alexis F, Pridgen E, Molnar LK, Farokhzad OC. Factors affecting the clearance and biodistribution of polymeric nanoparticles. *Mol Pharmaceutics*. 2008;5(4):505-515.

49. Arleth L, Xia X, Hjelm RP, Wu J, Hu Z. Volume transition and internal structures of small poly(N-isopropylacrylamide) microgels. *J Polym Sci B Polym Phys*. 2005;43(7):849-860.

50. Andersson M, Maunu SL. Structural studies of poly(N-isopropylacrylamide) microgels: Effect of SDS surfactant concentration in the microgel synthesis. *J Polym Sci B Polym Phys*. 2006;44(23):3305-3314.

51. von Nessen K, Karg M, Hellweg T. Thermoresponsive poly-(N-isopropylmethacrylamide) microgels: Tailoring particle size by interfacial tension control. *Polymer*. 2013;54(21):5499-5510.

52. Still T, Chen K, Alsayed AM, Aptowicz KB, Yodh AG. Synthesis of micrometer-size poly(N-isopropylacrylamide) microgel particles with homogeneous crosslinker density and diameter control. *J Colloid Interf Sci*. 2013;405:96-102.

53. López-León T, Ortega-Vinuesa J, Bastos-González D, Elaïssari A. Cationic and anionic poly(N-isopropylacrylamide) based submicron gel particles: Electrokinetic properties and colloidal stability. *J Phys Chem B*. 2006;110(10):4629-4636.

54. Sigolaeva LV, Gladyr SY, Gelissen APH, et al. Dual-stimuli-sensitive microgels as a tool for stimulated spongelike adsorption of biomaterials for biosensor applications. *Biomacromolecules*. 2014;15(10):3735-3745.

55. Wiese S, Spiess AC, Richtering W. Microgel-stabilized smart emulsions for biocatalysis. *Angew Chem Int Ed*. 2013;52(2):576-579.